

MICROCOPY RESOLUTION TEST CHART
NATIONAL BUREAU OF STANDARDS-1963-A

AFAMRL-TR-80-20

12



AD A 098 942

TORSO EXPERIENCED AERODYNAMIC FORCES EXPERIENCED DURING EJECTION

ARTHUR J. NESTLE

FEBRUARY 1981

DTIC
ELECTE
MAY 15 1981
S D
A

Approved for public release; distribution unlimited.

AIR FORCE AEROSPACE MEDICAL RESEARCH LABORATORY
AEROSPACE MEDICAL DIVISION
AIR FORCE SYSTEMS COMMAND
WRIGHT-PATTERSON AIR FORCE BASE, OHIO 45433

DTIC FILE COPY

81 5 15 060

NOTICES

When US Government drawings, specifications, or other data are used for any purpose other than a definitely related Government procurement operation, the Government thereby incurs no responsibility nor any obligation whatsoever, and the fact that the Government may have formulated, furnished, or in any way supplied the said drawings, specifications, or other data, is not to be regarded by implication or otherwise, as in any manner licensing the holder or any other person or corporation, or conveying any rights or permission to manufacture, use, or sell any patented invention that may in any way be related thereto.

Please do not request copies of this report from Air Force Aerospace Medical Research Laboratory. Additional copies may be purchased from:

National Technical Information Service
5285 Port Royal Road
Springfield, Virginia 22161

Federal Government agencies and their contractors registered with Defense Documentation Center should direct requests for copies of this report to:

Defense Documentation Center
Cameron Station
Alexandria, Virginia 22314

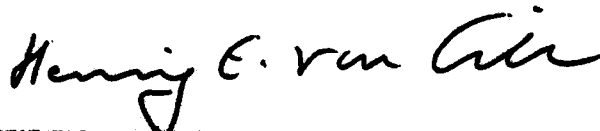
TECHNICAL REVIEW AND APPROVAL

AFAMRL-TR-80-20

This report has been reviewed by the Office of Public Affairs (PA) and is releasable to the National Technical Information Service (NTIS). At NTIS, it will be available to the general public, including foreign nations.

This technical report has been reviewed and is approved for publication.

FOR THE COMMANDER



HENNING E. VON GIERKE, Dr. Eng.
Director
Biodynamics and Bioengineering Division
Air Force Aerospace Medical Research Laboratory

(Line 20 Continued)

Since aerodynamic forces are related to aircraft proximity, a more anatomically localized understanding must necessarily be available to support biomechanical analysis of the ejection event.

To gain insight into operational injury, the McDonnell-Douglas F-4E aircraft was chosen, because of the available accident data base. A 1/32 scale model was constructed. The modelled crewmembers were machined to allow static porting at torso extremity locations of elbows, knees, top of the head and others. In addition, the model crewmembers were designed to be movable along an ejection path to four man-seat heights relative to the canopy-off fuselage rim: below, shoulder high, knee high and toe high. The aerodynamic data were obtained from tests in a five-foot wind tunnel and coefficients-of-pressure calculated from manometer readings.

These coefficients are determined for crewmember location and pitch and yaw trim of the aircraft from -10 to +10 degrees each and graphically analyzed using three-dimensional computer plots. Severity, gross kinetic changes, and points of force application are described.

SUMMARY

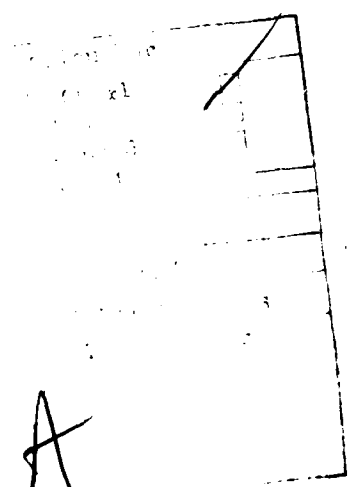
This investigation yielded some interesting findings on crewmember pressure coefficients, and subsequent aerodynamic forces experienced, during emergency egress.

The Weapons System Officer (WSO):

- Evidenced greater magnitude and more sporadic pressure coefficient than the pilot,
- Evidenced the greatest magnitude and intense rate of change pressure coefficient observed at the elbow,
- Evidenced at ejection greater upper torso loads than the pilot.

The Pilot:

- Helmet/head front had greater positive pressure coefficient environment than the WSO,
- Experienced decreased pressure coefficients with negative pitch trim.



PREFACE

This work was initiated under project 72311101, "Escape Injury Analysis." The author is assigned to the Biodynamic Effects Branch, Biodynamic and Bioengineering Division, Air Force Aerospace Medical Research Laboratory. The assistance of the Air Force Institute of Technology Zone Shop (Mr. Carl Short) and Wind Tunnel (Professor H. Larson and Misters Scott and Yardich) is appreciated.

TABLE OF CONTENTS

	Page
Introduction	5
Objective	5
Dynamic Similarity of Model	5
Materials and Methods	6
The Model	6
Pressure Ports	6
Positions	7
Method of Exact Positioning	10
Sequence of Test	10
Photographic Coverage	10
The Wind Tunnel	11
Sequence of Events (F4)	12
Data Reduction	12
Experimental Results	13
Weapons System Operator (WSO)	13
WSO, Summary	14
Pilot	16
Pilot, Summary	19
Comparison: Pilot - WSO	19
Operational Data	21
Appendix: Analytic/Graphic Data	29
References	44

LIST OF ILLUSTRATIONS

Figure	Page
1 Scale Model Construction Cut-Away	6
2 Pressure Port Locations, Crewmember Right Profile	7
3 Pressure Port Locations, Crewmember Left Profile	7
4 Test Positions, Weapons System Officer (WSO)	8
5 Test Positions, Pilot	9
6 Wind Tunnel Facility	11
7 Pressure Coefficient vs Position - WSO	14
8 Pressure Coefficient vs Position - WSO - $\pm 4^\circ$ pitch	15
9 Pressure Coefficient vs Position - WSO - $\pm 4^\circ$ pitch	15
10 Pressure Coefficient vs Position - Pilot	16
11 Pressure Coefficient vs Position - Pilot - $+ 10^\circ$ and $- 8^\circ$ pitch trim	17
12 Pressure Coefficient vs Position - Pilot - $+ 10^\circ$ and $- 8^\circ$ pitch trim	17
13 Operational Injuries	22
14 Head Anthropometry (for area)	23
15 Aerodynamic Loads, Pilot, 200KTS, Sea Level	25
16 Aerodynamic Loads, Pilot, 300KTS, Sea Level	25
17 Aerodynamic Loads, Pilot, 500KTS, Sea Level	26
18 Aerodynamic Loads, WSO, 200KTS, Sea Level	26
19 Aerodynamic Loads, WSO, 300KTS, Sea Level	27
20 Aerodynamic Loads, WSO, 500KTS, Seal Level	27
21 Knots vs Altitude (density) vs Dynamic Pressure (q)	28
22 Pressure Coefficients, Pilot, PP1	30
23 Pressure Coefficients, Pilot, PP2	31
24 Pressure Coefficients, Pilot, PP3	32
25 Pressure Coefficients, Pilot, PP4	33
26 Pressure Coefficients, Pilot, PP5	34
27 Pressure Coefficients, Pilot, PP6	35

LIST OF ILLUSTRATIONS (Continued)

Figure		Page
28	Pressure Coefficients, Pilot, PP7	36
29	Pressure Coefficients, WSO, PP1	37
30	Pressure Coefficients, WSO, PP2	38
31	Pressure Coefficients, WSO, PP3	39
32	Pressure Coefficients, WSO, PP4	40
33	Pressure Coefficients, WSO, PP5	41
34	Pressure Coefficients, WSO, PP6	42
35	Pressure Coefficients, WSO, PP7	43

LIST OF TABLES

Table		Page
1	Pressure Port Numeric Designations and Locations	7
2	Unit Magnitude of Absolute Change Over Four Positions	19
3	Maximum Pressure Coefficient Comparison	20
4	Aerodynamic Forces (psi) at Selected Airspeeds, Pilot	20
5	Aerodynamic Forces (psi) at Selected Airspeeds, WSO	20
6	Approximated Anthropometric Areas	24
7	Total Aerodynamic Load, Pilot	24
8	Total Aerodynamic Load, WSO	24

INTRODUCTION

Emergency egress exposes an aircrewman to abrupt accelerative and windblast forces. To shed further light on the magnitude and duration of aerodynamic loads experienced on various anatomical regions, a unique investigation was conducted, using a modified 1/32 scale model of the McDonnell-Douglas Corporation F-4E aircraft and crewmembers in wind-tunnel flow.

OBJECTIVE

The objective of this effort is to measure local pressure coefficients at selected anatomical areas of crewmembers and compare the results to man seat position for the pilot and WSO during the catapult phases of ejection for various aircraft trim conditions. The results are to be related to known injury modes.

DYNAMIC SIMILARITY OF MODEL

Wind tunnel models will not precisely reproduce actual aerodynamic conditions, nevertheless, it can be mathematically shown that nondimensional coefficients vary with scale effect (Taylor, 1925; Pankhurst, 1952). Relative difference¹ between coefficients of configuration changes and coefficients of the full scale configuration changes can be used in problem application, within experimental limits. From the literature, the degree of compatibility has been measured as 8% for the same Reynolds Number (Taylor, 1925) and 1% of the maximum variable (Owen, 1958).

Certain conditions must be met to optimize this agreement. The model must be geometrically similar to the prototype external shape (Pankhurst and Holder, 1952), and the density and the viscosity of the fluid must be alike. The tests most completely free of this "scaling" or Reynolds Number effect are pressure readings. This experiment, a pressure survey essentially, is in that group. This allows application of relative difference data to engineering problems involving incompressible flow.

¹ Difference due to small configuration change from an established aircraft/flow environment.

MATERIALS AND METHODS

The Model

A Revell Incorporated, #H 182, model was the beginning frame for the instrumented scale aircraft/crew. Crewmembers were 5 ft., 5 in. in height in the 1/32 scale.² This is a 5th percentile man (Grunhofer, 1975). The model was reinforced with epoxy resin and crew compartment retrofitted to allow man/seat movement into the windstream (Figure 1). The seat rail angle was engineered at 19° from vertical which is operationally correct for the (F4) Martin-Baker seat system. Figures 2 and 3 graphically display the location of aircrewmember static ports for scaled Pilot and WSO. Each scaled crewmember is identically ported. The port locations were chosen to provide data on areas of frequent operational injury/interest—the head/neck and the extremities. The cockpits were scaled from the aircraft body.

Pressure Ports

Pressure port locations are anatomically defined in Figures 2 and 3 for pilot and WSO. Numerically they are referred to as:

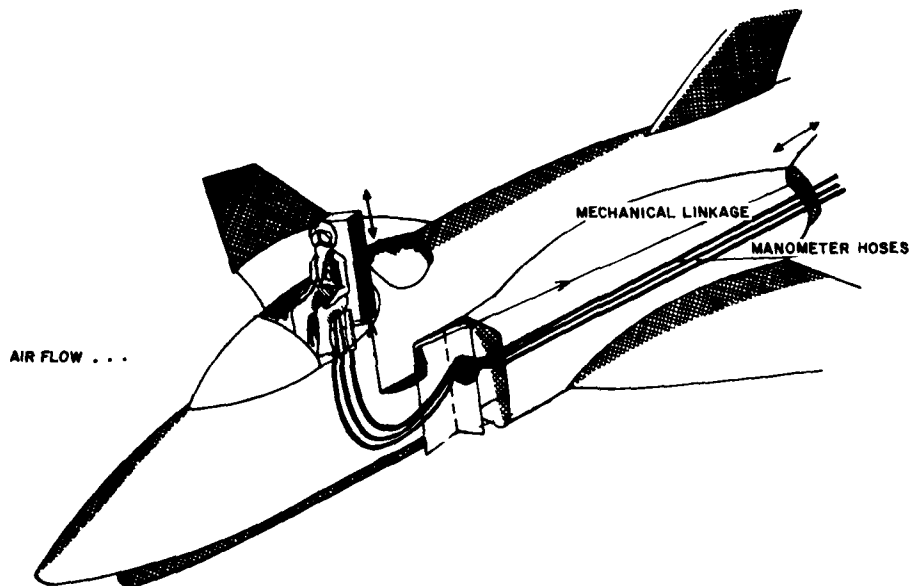


Figure 1. Scale Model Construction Cut-Away

²Cambell, R., Personal Communications, Revell Inc., Venice CA, 1979.

TABLE 1
PRESSURE PORT NUMERIC DESIGNATION AND LOCATIONS

<i>Number</i>	<i>Location</i>
PP1	Top of the helmet/head
PP2	Side (right) of the helmet/head
PP3	Front of the helmet/head
PP4	Elbow (left)
PP5	Knee, side (right)
PP6	Knee, front
PP7	Foot, toe

Each crewmember is identically instrumented.

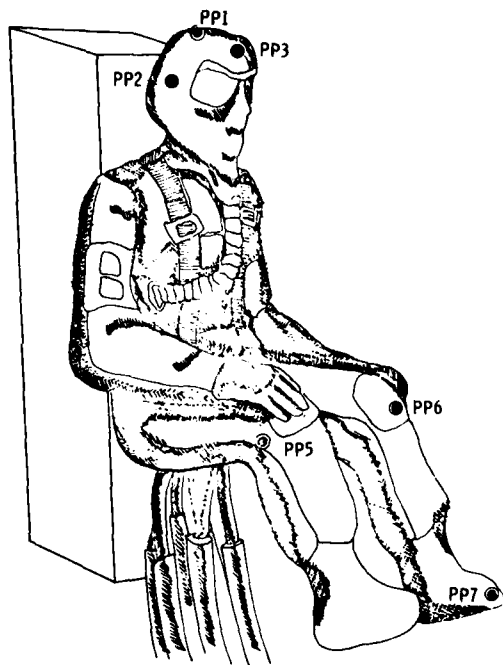


Figure 2. Pressure Port Locations, Crewmember Right Profile

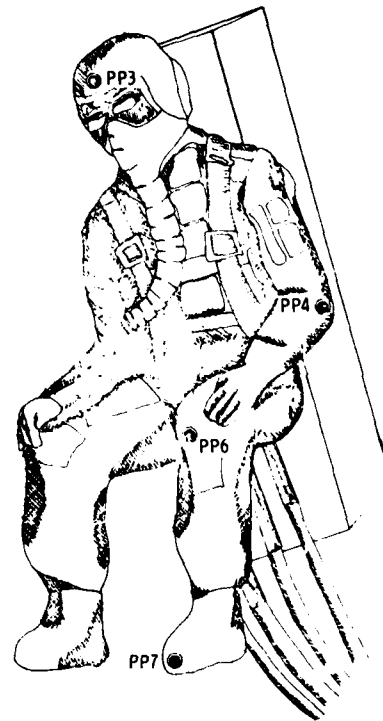


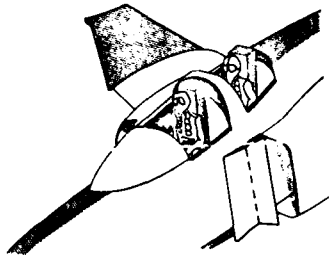
Figure 3. Pressure Port Locations, Crewmember Left Profile

Positions

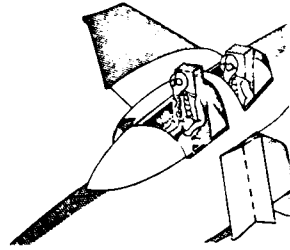
Crewmember positions are addressed in this report as P1, P2, P3 and P4 for the pilot and W1, W2, W3 and W4 for the WSO. The numeric suffix defines the crewmember location and is narratively described below and graphically portrayed in Figures 4a, b, c, and d for the pilot and Figures 5a, b, c, and d for the WSO.

Position 1. The crewmember is fully down in the cockpit. Crewmember placement was analytically derived from photo-analysis of the configuration of an operational aircraft (Figures 4a and 5a).

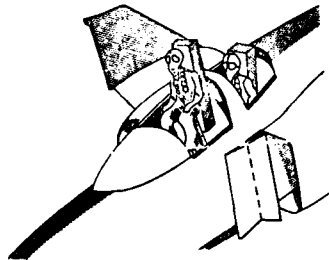
Position 2. The crewmember/seat combination is raised until the crewmember's shoulder, anatomically the region of deltoid muscle, was at the level of the front windscreen for the pilot and the limit of the canopy separation structure (hut) for the WSO (Figures 4b and 5b).



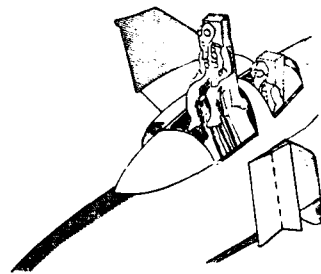
4a. P1, down in the cockpit



4b. P2, shoulder height

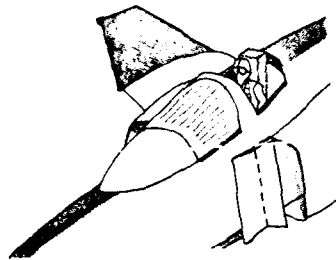


4c. P3, Knee height

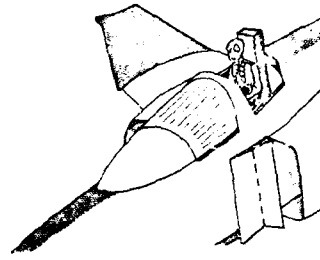


4d. P4, foot height, fully extended

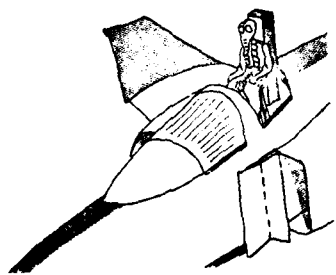
Figure 4. Test Positions, Weapons System Officer (WSO)



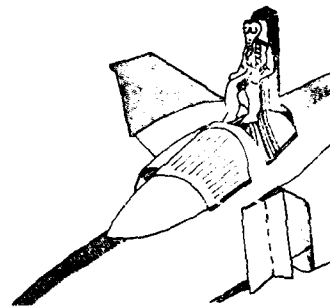
5a. W1, down in the cockpit



5b. W2, shoulder height



5c. P3, Knee height



5d. W4, foot height, fully extended

Figure 5. Test Positions, Pilot

Position 3. The crewmember's knee (patella) is brought even with the structures defined for P2 and W2 (Figures 4c and 5c).

Position 4. Position 4 is full extension. The crewmember is moved until the bottom of the foot is even with the structures defined for P2 and W2 (Figures 4d and 5d).

Method of Exact Positioning

For each aircrewman, the horizontal cross-hair of an ocular transit was sighted from outside the tunnel, through an observation port, and adjusted to measure a line level with the limit of the forward windscreen. Positions 2, 3 and 4 were established by advancing the crewmember until the anatomically located pressure port became level with the previously set horizontal cross-hair. Each position, 2 to 4, then reflects that anatomical segment at the same vertical height as the fuselage/canopy structure upstream of the flow. When pitch varied, the position was established then configuration change introduced.

As a result of aircraft design, the WSO is relatively higher than the pilot for comparable positions described.

Aircraft model pitch and yaw trim were set with a digital reading of cable setting on the sting,³ previously correlated to degrees by physically placing a precision liquid level on the longitudinal axis of the aircraft model and observing the measurement with respect to horizontal. Accuracy is ± 2 minutes of arc. The flow was confirmed uniform by previous tunnel calibration efforts (Haebec, 1955; Wood, 1957).

Sequence of Test

The tests were run at 130 mph. The decision for this value is addressed under the major section on wind tunnel. Tunnel speed was confirmed before and after each data record.

Experimentation followed this sequence:

- (a) Front canopy on, back canopy off;
- (b) WSO adjusted through positions W1-W4 and manometer readings photographed, WSO retracted (full down);
- (c) Aircraft trim angle changed in pitch, sequence item (b) repeated;
- (d) Aircraft trim angle changed in yaw, sequence item (b) repeated;
- (e) Front canopy off, back canopy off, both crewmembers retracted;
- (f) Pilot adjusted through positions P1-P4 and manometer readings photographed, pilot retracted;

Items (c) and (d) were accomplished for the pilot. Pitch trim nose up is considered to be positive. Yaw trim to the right is considered to be positive.

Photographic Coverage

Documentary 16mm movies were made of the wind tunnel test section with the model installed, wind tunnel operator station and instrumentation, mechanical leverage for moving crewmembers and fluid manometer board. Color still 35mm photographs also were taken of the scaled model mounted on the sting in the tunnel test section. Black and white 35mm, developed to 8 in. \times 10 in. size, were taken of the manometer board for every test condition measured. These were used in reducing the data.

³A sting is a horizontal and vertical yoke frame used for wind tunnel model mounting.

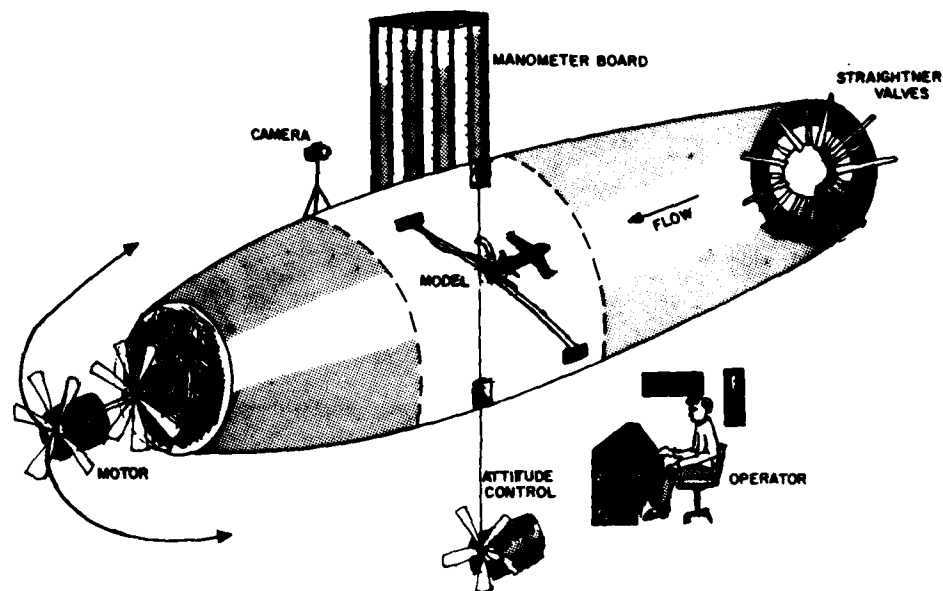


Figure 6. Wind-Tunnel Facility

THE WIND TUNNEL

The Air Force Institute of Technology Aero Design Center wind tunnel (Figure 6) is a low-speed, single-return-type; the building provides a double-return air passage. The tunnel working section is circular geometry of five feet diameter. The tunnel is vented to ambient pressure at the working section, establishing the pressure reference datum. Dynamic pressure ($q = \frac{1}{2} \rho V^2$) for the selected operating speed of 190.66 ft/sec (130 mph) was 43 PSF (lb/ft²). Tunnel and model pressures were photographed from a bank of manometers having a range of 60 inches fluid (SG = .6) displayed in 1/10th of an inch increments, interpreted to the 1/100th decimal place.

Wind tunnel tests to compare data were made at 130, 150, and 170 mph. The coefficients were calculated and compared. The variation of coefficients at like configuration with speed was no more than 3% of the largest value, over the 40 KT range. The lowest speed, 130 mph, was chosen for the test to reduce aerodynamic flailing of connecting hose and cable.

Force Measurement

For this purpose the normal pressure acting at the surface of the scaled crewmembers is measured at a number of holes drilled normal to the surface and fitted with 0.04 diameter hypodermic tubing.

SEQUENCE OF EVENTS (F4)

In a sequenced operational ejection from the F4 aircraft, the events are:

- WSO canopy separates
- WSO seat functions/WSO egress
- Pilot canopy separates
- Pilot seat functions/pilot egress

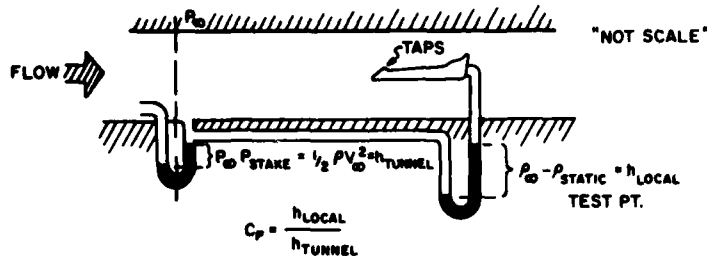
Individually, each crew location sequence is:

- canopy jettison
- inertia reel retracts
- ejection gun fires
- seat is propelled up guide rails

DATA REDUCTION

The pressure coefficient, C_p , is obtained directly as a ratio of the manometer readings, corresponding to tunnel pressure, p , and to dynamic pressure, $\frac{1}{2} V^2$, being given by a pilot-static tube in the working section upstream of the model (i.e., tunnel "q"). Fluid height was determined to the 1/100 position using a magnifying lamp. These values comprised the fluid differential values used in calculating the pressure coefficients. Calculated values for all crewmember positions and aircraft trim variations are the Appendix.

Coefficient measurement is shown here:



$$C_p = \frac{h_{\text{tube local}}}{h_{\text{tunnel "q" tube}}} \quad (1)$$

h - fluid height
p - pressure

Pressure port locations are shown in Figures 5 and 6.
Force calculations were uniquely determined from:

$$F = C_p \frac{1}{2} \rho V^2 S \quad (2)$$

- C_p - experimentally determined local pressure coefficient (Figures A1-A14)
- ρ - local density of air (slugs/ft³), an altitude function
- V - aircraft velocity (ft/sec)
- S - area (ft²), when taken as 1/144, F has units of pounds per square inch, psi.

Equation 2 shows that ρ and V are the only variables dependent on ejection environment. Therefore, the general trend of increasing local aerodynamic forces with increasing airspeed; and increasing local aerodynamic force with decreasing altitude, is observed in Figure 21. Results of applying formula (2) are presented in Tables 4, 5, 7 and 8 and Figures 15 through 20.

EXPERIMENTAL RESULTS

The data are discussed in order of crewmember static port location. Negative (-) pressure is localized "pull" or lift. Positive (+) pressure is experienced as "push." The Appendix contains the entire analytical coefficients.

Weapons System Operator (WSO)

PP1 (the top of the helmet/head) displays a negative pressure coefficient which increases with uniformity as the man/seat moves to full extension, when a reduced coefficient rate of increase is observed (Figure 7). The value of the coefficient increases to six times its original measurement during the position change. In a yaw trimmed situation, the WSO port PP1 displays a decreasing pressure coefficient with negative (nose down) pitch trim.

The side of the helmet (PP2) exhibits a pressure coefficient of similar graphic appearance as at the top of the helmet/head. Because of the geometric resemblance of the helmet/head to a sphere, these two pressure port locations would be expected to experience a similar flow environment. The side helmet/head pressure coefficient is maximum before the scaled man/seat is fully involved with the flow. The pressure coefficient is calculated at $-.691$ (Figure A9) for position 3 (knees at the canopy hut) and reduced to $-.561$ at position 4 (feet at the canopy hut). Port PP2, the right side of the helmet/head, confirms the asymmetry of location. For 0° yaw trim, the coefficient decreases with negative pitch trim. The coefficient increases with positive yaw trim changes when the aircraft is trimmed in pitch.

The front of the head/helmet (PP3) evidences a large magnitude positive pressure coefficient. A small magnitude when the WSO/seat is fully within the fuselage (W1), the pressure load establishes rapidly and exhibits the maximum value after position W2 (shoulders at canopy hut). Subsequently, this coefficient decreases by .35, almost 50%. It is hypothesized that this reflects the increased dynamic pressure component near the scale model and reduced dynamic pressure in the established field a distance away. The rate of change of the pressure coefficient is very high. The front of the helmet/head displays an increased coefficient with nose down trim in all positions.

The elbow (PP4) experienced a negative pressure coefficient of greatest magnitude. This was between positions 2 and 3. Initially, that coefficient is .005 and very shortly thereafter is measured to be -2.054 (Figure 32). This is a substantial value, operationally manifested in an intense force pulling the elbow away from the torso. The coefficient rate of change is virtually instantaneous. The maximum magnitude, reached at position W3 (knees level with the canopy hut), is -2.054 . At 0° and $+4^\circ$ pitch trim and with $+4^\circ$ yaw trim (Figure 9) the value is greater, -2.249 and -2.299 respectively. As the crewmember seat model is totally involved in the flow the coefficient decreases (for a trimmed condition) to -1.707 . This port evidences turbulent coefficient values. Positive yaw trim creates large measurements at position 4. Position 3 evidences response to positive yaw trim by producing large coefficient values.

The knee side evidences small pressure coefficient increases for positions until beyond the canopy hut, where greater coefficient values are observed to a maximum value of $-.293$ (Figure A12) when fully extended.

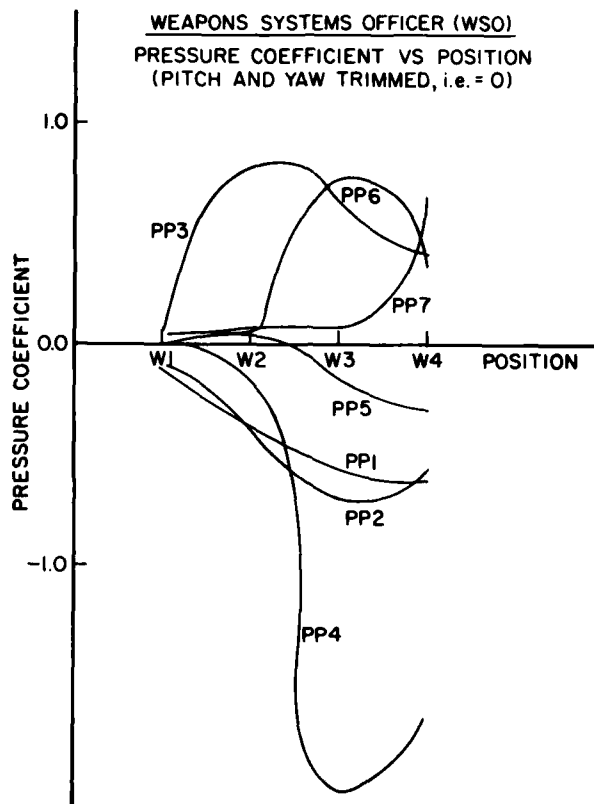


Figure 7. Pressure Coefficient vs Position, WSO

A coefficient of .775 (Figure 34) is measured when the front of the knee is positioned level with the canopy hut. A reduction to .356 occurs when the crewmember is fully extended. At positions 1 and 2 small coefficients are calculated. The rate of change between positions 2 and 3 is large, decreasing after position 3. The front of the knee (PPG) increases in value of calculated pressure coefficient as pitch decreases. It evidences an asymmetry with large coefficients in positive yaw trim conditions.

The front of the foot (PP7) has low positive pressure coefficient values (Figure 35) before moving beyond the cockpit structure when a very high rate of change is observed as the WSO/seat becomes fully involved with the flow, when a maximum value of .571 is calculated. A high rate of change still exists at position 4, indicating a trend for continued increase. Increasing coefficient with negative pitch is also observed for all values.

WSO, Summary

The elbow experienced the largest magnitude pressure coefficient and the greatest rate of coefficient change. The maximum value (negative) was twice the magnitude of any other region observed, manifesting frequent operational injuries. The rate of change was severe and created a "jerk" on the extremity. Except for the top of the head, side of the knee and front of the foot, the measured locations exhibited a reduction from maximum value observed when fully enveloped by the flow. The front of the knee and front of the helmet/head evidenced this reduction near position W3. The reduction represents a smaller dynamic pressure, therefore reduced flow velocity. The WSO crewmember evidences a disturbed, turbulent flow pattern except very near the fuselage where more predictable flow is observed. The energy lost to turbulence is reflected in reduced velocity, and therefore reduced dynamic pressure. The side of the knee (Figure 20) is the only anatomical location experiencing a changed pressure coefficient value that is originally positive (.01 at position W1 and .044 at position W2) and changes to negative (-.167 and -.293) at more extended crewmember/seat positions.

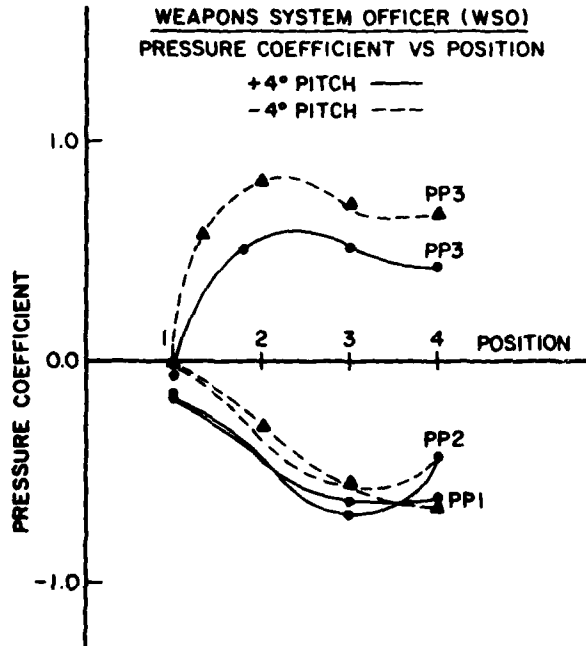


Figure 8. Pressure Coefficient vs Position, WSO, Changing Pitch Trim

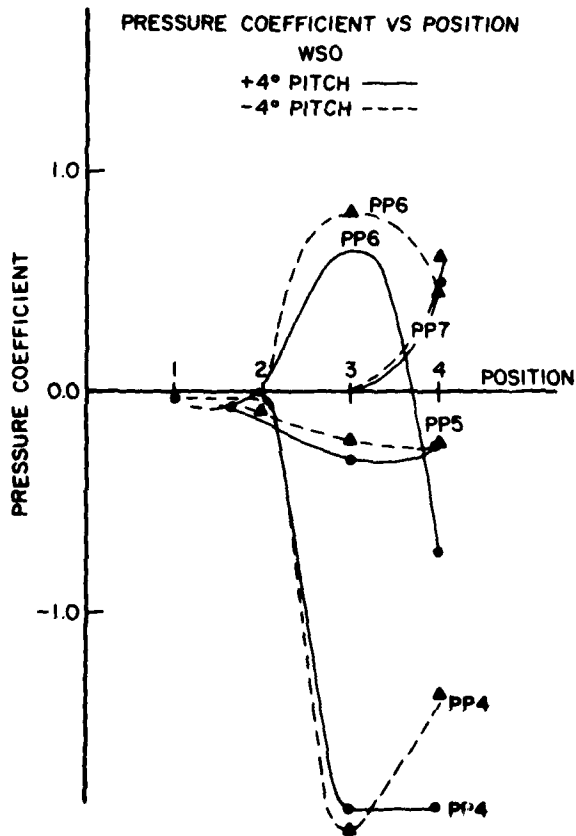


Figure 9. Pressure Coefficient vs Position, WSO, Changing Pitch Trim

Pilot

The positions along the trajectory previously defined and reflected in Figure 10 are for the seven unique anatomical locations of pressure port placement.

For PP1, the coefficient value is -0.185 (Figure 22), the largest measured on this crewmember at the P1 position. The coefficient increases in a uniform negative gradient with entry into the flow field. The increase is maximum at P4 position. That value is -0.451 . This coefficient almost doubles while the pilot is moving from the lowest cockpit position (P1) to fully involved (P4) with the airstream, which operationally takes place over 0.25 second. It has the effect of placing the head/neck/spine in tension. Negative pitch trim (nose down) decreases the measured pressure coefficient at positions P2 and P3. For P4 and 0° yaw trim, the PP1 coefficient increases with negative pitch trim. Position P4 displayed the largest coefficient values measured at the top of the helmet/head.

The side of the helmet (PP4) - and for a 0° yaw trim condition this reflects both sides - evidences slight negative pressure when the crewmember is fully down. As the pilot is raised to a position of shoulder's level with the fuselage rim, a negative increase is evidenced. The coefficient value continues to increase in a negative magnitude uniformly once the helmet/head have been inserted in the airstream. As seen in Figure 10, the rate of negative increase of this side coefficient is similar to the helmet top pressure port location. This is a reflection of the spherical geometry of the flight helmet. The side experiences a greater dynamic pressure possibly because of the streamlining effect the front canopy screen has on the flow. The onset of these loads takes place in about one foot of rail travel. The side of the helmet/head port, PP2, reflects asymmetry of location (i.e., the port is on the right side of the modeled crewmember). Negative yaw trim universally reflects a larger magnitude pressure coefficient than neutral trim or positive yaw trim (Figure 11). Yaw at 0° trim and negative pitch trim (nose down) result in decreased pressure coefficient for P2 and P3. At P4, the effects of pitch variation is random.

The helmet/head front pressure port (PP3) measures positive coefficient values, effectively "pushing" the helmet/head back into the headrest. The measured coefficient is greater as the helmet/head initially engages the stream flow then

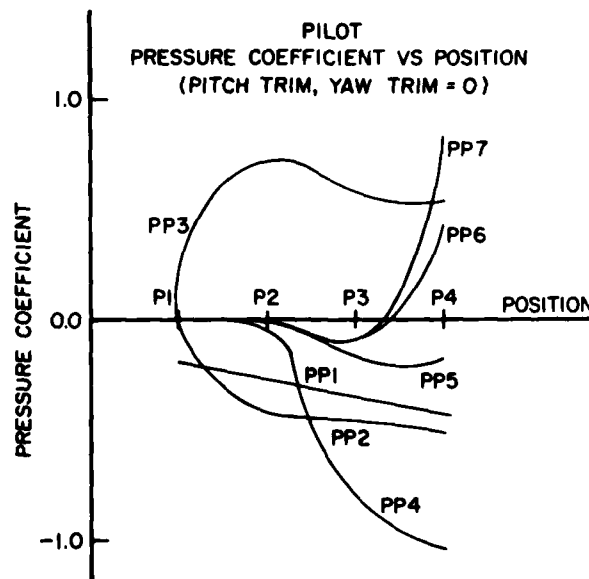


Figure 10. Pressure Coefficient vs Position, Pilot

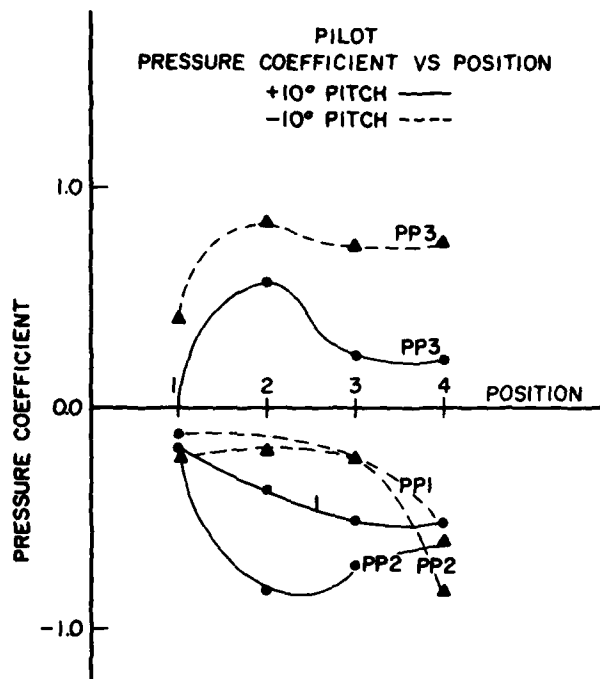


Figure 11. Pressure Coefficient vs Position, Pilot, Changing Pitch Trim

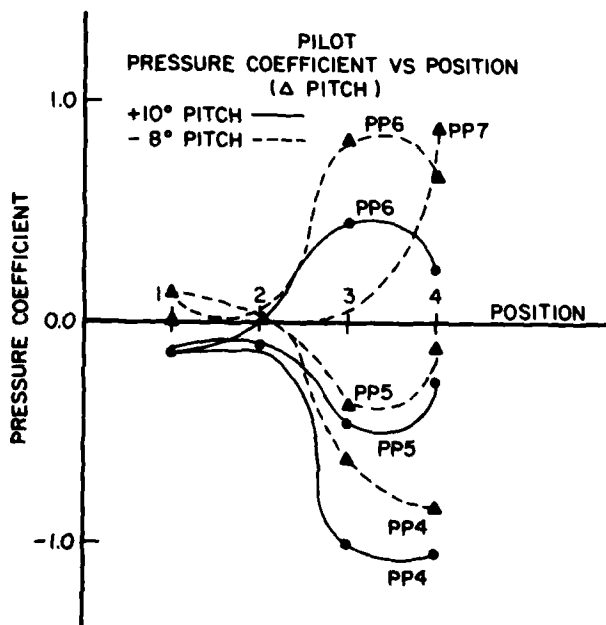


Figure 12. Coefficient vs Position, Pilot, Changing Pitch Trim.

declines as the man/seat are at position P4. This supports the hypothesis of a greater dynamic pressure near the fuselage. The frontal port (PP3) displays an increased magnitude of coefficient for decreasing values of pitch trim. The coefficient at PP3 is relatively unchanged in yaw trim.

The helmet/head/neck were observed to experience tensile force resulting from aerodynamic loading of the helmet top, immediately after canopy separation. At that time, this was the greatest aerodynamic force experienced by the pilot. As movement up the rail puts the helmet/head into the flow, simultaneous loading of the front and sides occurs. The negative gradient of the side coefficient materializes after the positive coefficient of the front. Front to back helmet/head force happens at position 1 and is of large magnitude. Side loading is achieved at a lesser rate and smaller magnitude. Asymmetrical entry into the flow can be investigated by observing the response to yaw trim (Figure 23). Fully extended into the stream and trimmed in pitch (0°) with -4° yaw, the upstream side of the helmet experiences a $-.447$ coefficient. The downstream side views a pressure coefficient of $-.852$. This differential is twice the symmetrical load condition and creates a lateral force on the head/neck, increasing as a function of velocity. The elbow (PP4) experiences very large negative values. As the man/seat moves up the rails, with the shoulder approaching the fuselage rim (P2), the steep coefficient gradient is even more intense (Figure 25). This coefficient value did not respond like those from the helmet but continues to increase until equal to the largest negative coefficient measured for the pilot, -1.203 (0° pitch and 0° yaw). This load is observed to be of a high rate of application. The possibility of trauma at the elbow cannot be over-emphasized in light of magnitude and rate of change over a very short time span. Pitch trim nose-down reduces the measured pressure coefficient at the four positions of this investigation (Figure 12). Pressure coefficient calculation of 0.0 is at -8° pitch trim, for position P2. Stagnation on the fuselage effectively causes the flow to recede from the geometric limits of the man/seat/fuselage section. The pilot is essentially not in the flow. The flow presents a geometry not identical to the model which affects the crewmember. The coefficient at the pilot's elbow (PP4) reflects a decreasing trend for 0° yaw trimmed and nose-down pitch changes (Figure 25). The asymmetry of location does not reflect in the coefficient versus yaw comparison, as at PP2.

The side of the knee (location PP5) evidenced the smallest pressure coefficient measured when the aircraft is trimmed. Any extreme of pitch trim ($+10^\circ$ or -8°) produces a greater negative coefficient at this anatomical location than trimmed (Figure A5). This reflects the magnitude of the nonhorizontal component of flow near the fuselage, to which the side of the knee is in close proximity. As the crewmember progresses up the rails, readings at the knee side increase before position 3 and are maximum at some time after the knee is fully involved, but before position 4. The frontal geometry of the scaled crewmember could cause the flow pattern past this anatomical location—a condition not existing at the helmet/head where greater coefficient values are measured. Flow stagnation at the frontal seat/man location forces the freestream around the blockage. Within this stagnation effect, significant reductions of flow velocity exist and this may be the manifestation experienced by the knee side (PP5). Figure 26 displays a decreasing pressure coefficient with negative pitch trim. The asymmetry of the knee side location is evident with increasing values of coefficient as positive yaw trim increases.

The front of the knee (PP6) experiences an intense aerodynamic force environment exhibiting negative and positive pressure characteristics (Figure 27). As the crewmember's shoulders pass the canopy hut, the front of the knee experiences negative pressure. This is maximum at position 3, whereafter, intense positive pressure is encountered. This tends to indicate that the flow field is just slightly beyond the structural limits of the scaled fuselage of the aircraft. When the man/seat are fully extended (position 4), the coefficient measured at the front of the knee is nearly equal to that at the front of the helmet/head (PP3). Establishment of the aerodynamic conditions precipitating this large local positive pressure measurement is very rapid. The force changing from a small negative pressure to a large positive pressure value is a condition not observed in the pilot's helmet/head or upper torso pressure port locations, but repeated at the foot/toe. This phenomenon of changing pressure from negative to positive with advancing position is only exhibited by the lower extremities of the pilot. For positions P3 and P4 the port at the front of the knee measured increasing coefficient values with nose-down (negative) trim. When fully raised into the flow, a large response to yaw trim is evidenced by this pressure port. At 0° pitch trim a pressure coefficient value of $-.018$ is calculated for -6 degrees yaw trim. At positive 8° yaw trim the pressure coefficient is $.634$.

PP7 location, at the toe, exhibited characteristics similar to the knee front but with greater final magnitude (Figure 10). For positions P1, P2 and the position of knee level with the fuselage, P3, the foot exhibits pressure coefficient values almost equal to the front of the knee. A difference results when the man/seat are fully into the flow and the pressure coefficient measured at the toe of the foot is twice that of the front of the knee. The measured coefficients at PP7 decrease with nose-up (positive) pitch trim.

TABLE 2

UNIT MAGNITUDE OF ABSOLUTE CHANGE OVER FOUR POSITIONS

PP Location	Crewmembers' Changes		Crewmembers Difference
	WSO	Pilot	
1	.60	.25	WSO, .35 greater
2	.70	.50	WSO, .2 greater
3	.80	.70	WSO, .1 greater
4	2.00	1.05	WSO, .95 greater
5	.30	.20	WSO, .1 greater
6	.75	.50	WSO, .25 greater
7	.70	.95	Pilot, .25 greater

Pilot, Summary

The front of the helmet, the elbow and the front of the foot exhibited the largest magnitude pressure coefficients. Except for the elbow, which is negative, the coefficient values indicate pushing. The elbow was exposed to a pull or lift environment. The lower extremities (knee and foot) and elbow evidenced very large coefficient changes with position change of the crewmember/seat. The front of the helmet/head also experienced large coefficient changes with movement and also very large magnitude for three of the measured locations of increasing exposure (P2, P3, P4). The greatest pressure coefficient was observed for the elbow at position 4. Table 4 displays calculated aerodynamic forces in pounds per square inch for selected airspeeds, at sea level, using the pressure coefficients measured during this investigation.

Comparison: Pilot - WSO

Table 2 is a comparison in units of absolute pressure coefficient change, from least to greatest measured value, for each of the seven pressure port locations. Below the designation of crewmember is the numeric value for the total absolute pressure coefficient change experienced at that anatomical location. The third column calls out the crewmember experiencing the greatest absolute difference from position 1 to 4 and includes the value of that *difference from the other crewmember*. This change in magnitude is addressed as it bears on the anatomical structure's ability to remain mechanically within failure limits.

The maximum pressure coefficients experienced are presented in Table 3. The location of the port is reiterated with corresponding crewmember experiencing the force, the value of the maximum pressure coefficient measured and the *difference that value is from the other crewmember*. The extreme values are of the same arithmetic sign for each crewmember; therefore, the difference is presented as the absolute magnitude from 0.0. The elbow of the WSO is unique in rate of pressure coefficient change and large maximum value achieved. It is .851 greater than the pilot experiences. It changes .95 more than the pilot. Because Figure 10 indicates the PP4 measurements on the pilot decreasing in rate of change, the large magnitudes experiences by the WSO are unlikely to be equalled. The maximum value is experienced by the WSO while the man/seat combination is less than fully involved with the flow, i.e., the seat still affixed to the rails in an operational situation. The WSO experiences greater changes in helmet/head coefficient values (Table 2) than the pilot. Specifically, the top of the head/helmet (PP1) is the second largest (+ 0.35) unit difference measured.

The side and front of the helmet/head model have smaller differential values of comparison, 0.2 and 0.1 respectively. The difference of maximum measured coefficient is only 0.046 for the side of the helmet/head. This is the closest value to identical extreme values by both crewmembers. The pilot evidences a greater coefficient (+ 0.550) at the front of the helmet/head than the WSO (+ 0.40). Overall the WSO evidenced a more diverse reading of pressure coefficients for the positions that would indicate the probability of turbulent aerodynamic loads operationally. The pilot measured greater

TABLE 3
MAXIMUM PRESSURE COEFFICIENT COMPARISON

<i>Location</i>	<i>Crewmembers</i>	<i>Value</i>	<i>Difference</i>
Helmet/head, top	WSO	-.629	.178
Helmet/head, side	WSO	-.561	.046
Helmet/head, front	Pilot	+.550	.150
Elbow	WSO	-.2.054	.851
Knee, side	WSO	-.293	.123
Knee, front	WSO	+.775	.332
Foot, toe	Pilot	+.841	.270

TABLE 4
AERODYNAMIC FORCES AT SELECTED AIRSPEEDS

		PILOT						
		Force (psi)						
<i>Velocity (KTS)</i>	<i>Altitude (FT)</i>	<i>Elbow</i>	<i>Knee, Side</i>	<i>Knee, Front</i>	<i>Toe</i>	<i>Head</i>		
						<i>Top</i>	<i>Front</i>	<i>Side</i>
200	SL	-1.17	-.16	.41	.78	-.43	.51	-.44
300	SL	-2.64	-.36	.91	1.76	-.96	1.15	-1.09
500	SL	-7.33	-1.01	2.54	4.88	-2.66	3.20	-3.03
200	10,000	-.87	-.12	.30	.58	-.31	.38	-.36
300	10,000	-1.95	-.27	.68	1.30	-.71	.85	-.81
500	10,000	-5.42	-.75	1.88	3.60	-1.96	2.37	-2.24
200	20,000	-.63	-.09	.22	.42	-.23	.27	-.26
300	20,000	-1.41	-.19	.49	.94	-.51	.62	-.58
500	20,000	-3.91	-.54	1.35	2.60	-1.42	1.71	-1.62

TABLE 5
AERODYNAMIC FORCES AT SELECTED AIRSPEEDS

		WSO						
		Force (psi)						
<i>Velocity (KTS)</i>	<i>Altitude (FT)</i>	<i>Elbow</i>	<i>Knee, Side</i>	<i>Knee, Front</i>	<i>Toe</i>	<i>Head</i>		
						<i>Top</i>	<i>Front</i>	<i>Side</i>
200	SL	-1.61	-.28	.34	.54	-.59	.38	-.53
300	SL	-3.62	-.62	.76	1.21	-1.33	.86	-1.19
500	SL	-10.06	-1.72	2.10	3.36	-3.71	2.38	-3.30
200	10,000	-1.19	-.20	.25	.40	-.44	.28	-.39
300	10,000	-2.67	-.46	.56	.89	-.99	.63	-.88
500	10,000	-7.43	-1.27	1.55	2.48	-2.74	1.76	-2.44
200	20,000	-.86	-.15	.18	.29	-.32	.20	-.28
300	20,000	-1.93	-.33	.40	.65	-.71	.46	-.63
500	20,000	-5.36	-.92	1.12	1.79	-1.76	1.27	-1.98

front (PP3) helmet/head coefficients than the WSO as the side helmet/head coefficients, and (0.178, Table 3) reduced top of the helmet/head coefficient. In aerodynamic terms, this means the pilot is pushed into the seat/helmet box with greater force. At the same time the pilot experiences less vertically upward force on the helmet/head than the WSO. The knee (front and side) of the WSO evidences greater coefficients (Table 2) and larger changes (Table 3) in coefficient than the pilot. The greatest difference in extreme value is at the knee front, where the WSO had a calculated coefficient of +0.775. This is +.332 greater than the pilot and a difference of change, with position, of .25 greater.

The pilot evidenced greater, +0.841 (Table 3), toe pressure coefficients and a more diverse pattern (Table 2) than the WSO. A comparison of Figure 6 with Figure 15 reflects this difference for PP7. The pilot evidences an initial negative pressure coefficient which changes to a positive value subsequent to position 3 and achieves .841 at position 4. Position 4 pressure coefficient for every WSO anatomical location is less than the maximum achieved except for the foot, while increasing coefficient values are displayed by the pilot for every pressure port except the front of the helmet/head for each position, *including* position 4. This indicates the WSO is seeing a more reduced velocity field at position 4 than the pilot and, in an operational situation, experiences extremes of aerodynamic force sooner after ejection. The WSO is in an environment of greater magnitude coefficients and greater rate of coefficient change than the pilot.

OPERATIONAL DATA

Figure 13 reflects the anatomical location and frequency of windflail injuries for all models of the F4 aircraft for the period 1967-1977 (Combs, 1979). In addition, Kazarian and Belk (1980) reported a single fatal cervical injury attributed to windblast in the F4 during ejection. Combs (1979) reported an overall F4 injury rate of 4.7%, resulting from windblast. The frequency, 39% (from Figure 13), of upper extremity flail injury reflects the magnitude and severity of change evidenced by the pressure coefficient measured in this investigation and force calculations at the elbow. The high on-set rate of this loading can predispose hyperextension of the elbow or hyperabduction of the shoulder, both identified as primary to injury at these locations.

Lower extremity injuries, 23% (from Figure 13), are caused by an aerodynamic environment that changes at a high rate as the crewmember leaves the protection of the forward fuselage/canopy structures. *Injury etiology for the lower extremities* has the limbs being forced outward (negative pressure on the knee side) and backward (positive pressure on the knee front) where they are either arrested by the seat structure or limit of travel of the body joint.

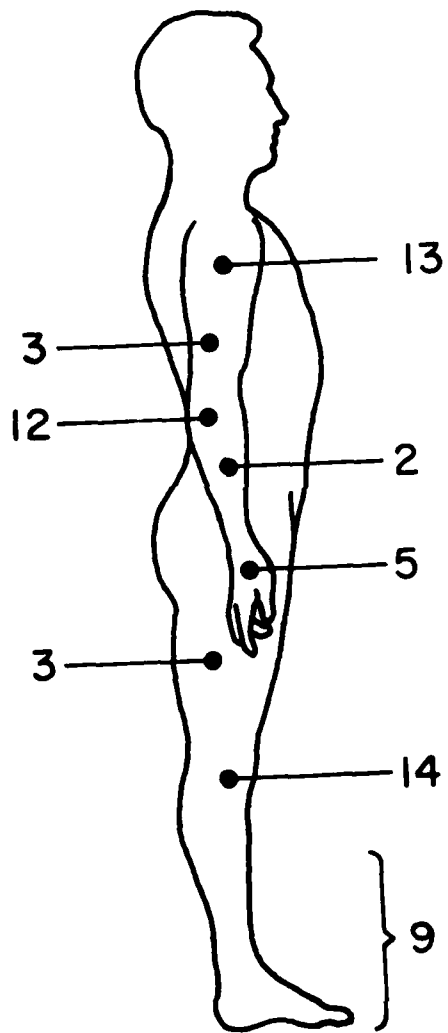
The head/neck is subjected to vertical "pull," sideward "pull" and frontal "push" aerodynamic loads. The result of these conditions is cervical spine hyperextension due to negative pressure on the helmet/head top, a force back into the headrest and possible lateral loading if the crewmember is not encountering the airstream symmetrically. Rotating displacement (Kazarian and Belk, 1980) of the vertebral joint results from intense asymmetrical loading. This is most always fatal.

These coefficient data address aerodynamic loads: (1) in close proximity to the aircraft, (2) while the crewmember/seat is still restrained by the rails, and (3) with the operational condition of upward velocity/acceleration not present.

In a +10° pitch trim, the side of the pilot's helmet/head shows an increase in pressure coefficient measured, especially at positions P2 and P3. The front of helmet/head load decreases with positive pitch trim and increases with negative trim. The pilot's foot was not affected by pitch trim but the front of the knee evidenced increased pressure measurement at P3 position.

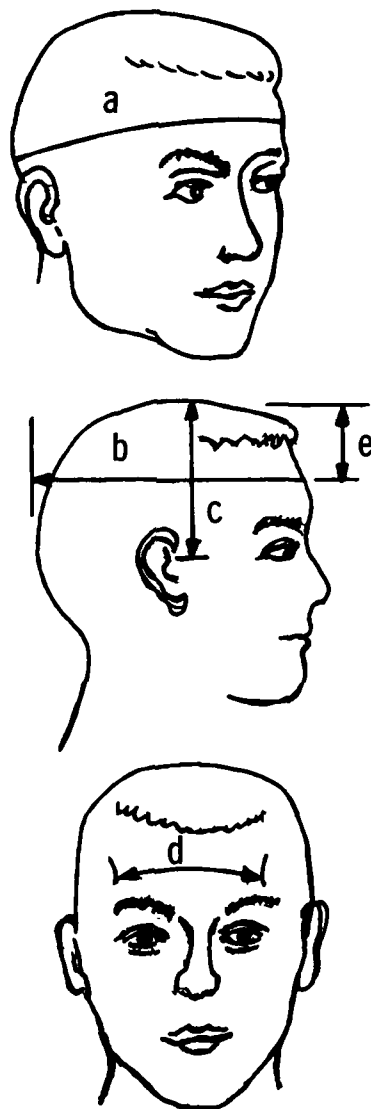
The WSO helmet/head did not show response to pitch trim from +10° or -8°. The front of the knee oscillated from positive to negative pressure between positions W3 and W4 at a trim of +4° pitch. This was not observed at -4° or 0° pitch trim.

To provide an appreciation of the total aerodynamic load experienced at any anatomical location, the localized values in Tables 4 and 5 were calculated for positions 4. Table 6, in conjunction with Figure 14, displays the approximated areas determined for each pressure port location. Formula 2, previously defined, was used. The results of this calculation are presented in Tables 7 (for the pilot) and 8 (for the WSO). These calculated values also appear on the crewmembers in Figures 15-17 and 18-20. The magnitude of local forces at higher airspeeds is remarkable.



TOTAL INJURIES: 95

Figure 13. Operational Injury (Combs, 1979)



- a. Maximum circumference of head
- b. Glabella to wall
- c. Tragon to level of top of head
- d. Bony points of brow ridge
- e. Glabella to top of head

Figure 14. Head Anthropometry for Area

TABLE 6
APPROXIMATE ANTHROPOMETRIC AREAS

<i>PP</i>	<i>Calculations of Approximated Area¹</i>	<i>Area (Square Inches)</i>
1	The maximum head diameter, squared. From measurement a, Figure 14.	51.33
2	Figure 14, measurement c multiplied by measurement b.	39.6
3	Figure 14, measurement d multiplied by measurement e.	18.27
4	The diameter of the elbow squared.	11.12
5	The diameter of the knee squared.	22.61
6	Same as PP5	22.61
7	Width protrusions of medial and lateral ankle bones, squared.	9.19

¹ All basic anthropometry, such as maximum head diameter or ankle width, was taken from Grunhofer and Kroh. The mean value was used.

TABLE 7
TOTAL AERODYNAMIC LOAD

		PILOT						
		Force (psi)						Head
<i>Velocity (KTS)</i>	<i>Altitude (FT)</i>	<i>Elbow</i>	<i>Knee, Side</i>	<i>Knee, Front</i>	<i>Toe</i>	<i>Top</i>	<i>Front</i>	<i>Side</i>
200	SL	- 13.01	- .36	9.27	7.16	- 22.07	9.31	- 17.42
300	SL	- 29.35	- 8.13	20.57	16.17	- 49.27	21.01	- 19.91
500	SL	- 81.50	- 22.8	57.42	49.48	- 136.53	58.46	- 55.36

TABLE 8
TOTAL AERODYNAMIC LOAD

		WSO						
		Force (psi)						Head
<i>Velocity (KTS)</i>	<i>Altitude (FT)</i>	<i>Elbow</i>	<i>Knee, Side</i>	<i>Knee, Front</i>	<i>Toe</i>	<i>Top</i>	<i>Front</i>	<i>Side</i>
200	SL	- 36.40	- 6.33	7.68	4.96	- 30.28	6.94	- 20.98
300	SL	- 81.85	- 14.02	17.18	11.2	- 68.76	15.71	- 47.12
500	SL	- 227.45	- 38.88	47.48	30.87	- 190.43	43.48	- 130.68

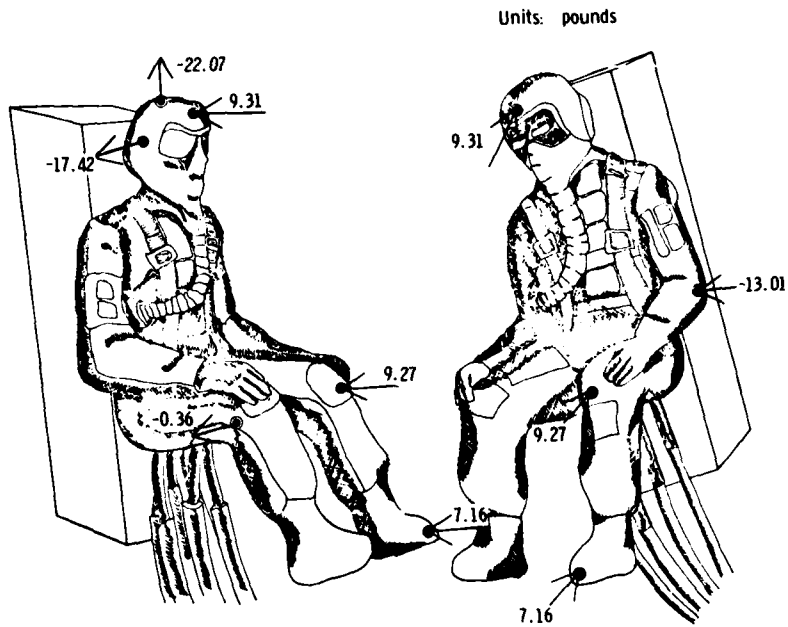


Figure 15. Aerodynamic Loads, Pilot, 200 KTS, Sea Level

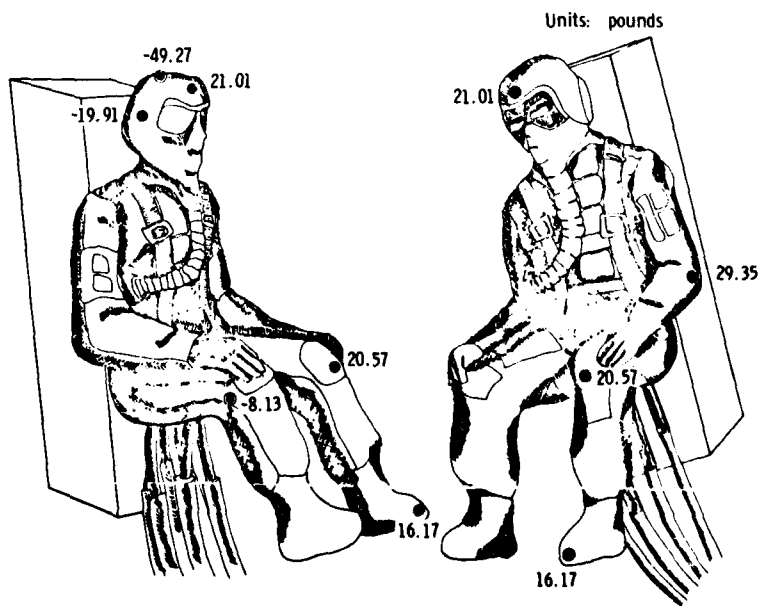


Figure 16. Aerodynamic Loads, Pilot, 300 KTS, Sea Level

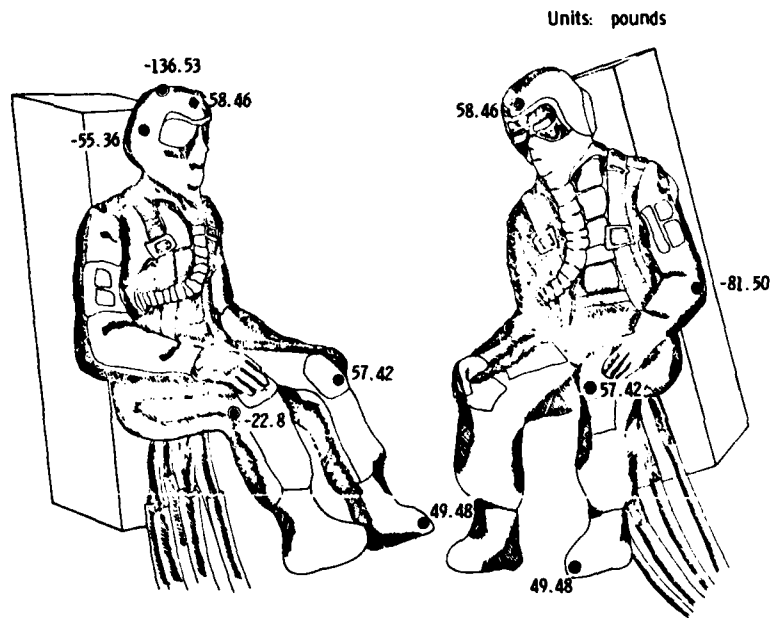


Figure 17. Aerodynamic Loads, Pilot, 500 KTS, Sea Level

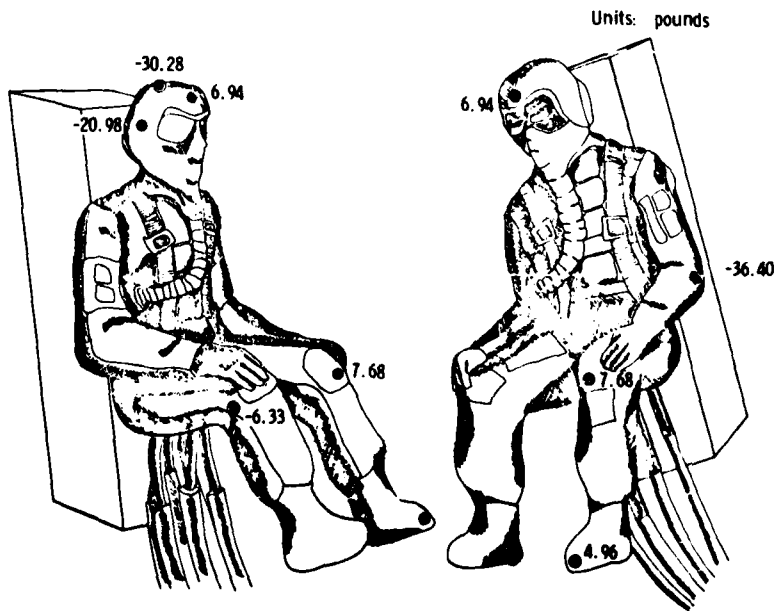


Figure 18. Aerodynamic Loads, WSO, 200 KTS, Sea Level

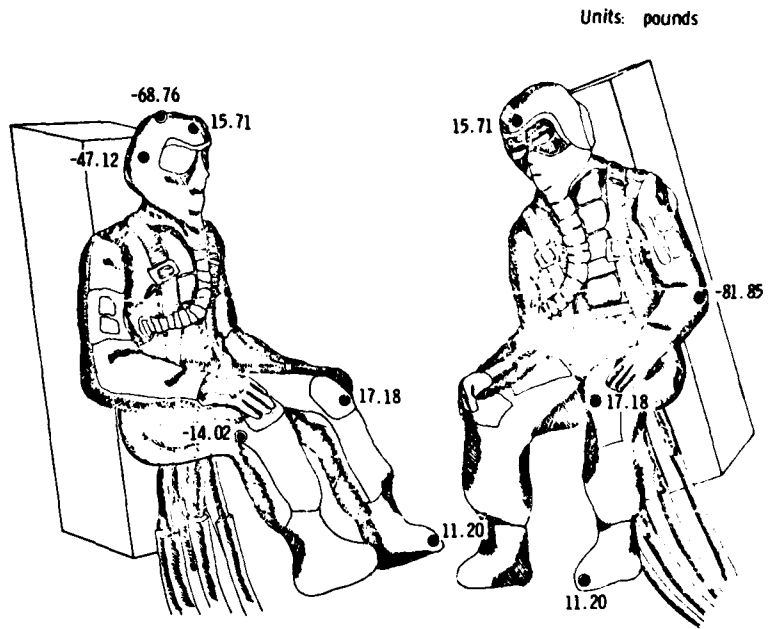


Figure 19. Aerodynamic Loads, WSO, 300 KTS Airspeed, Sea Level

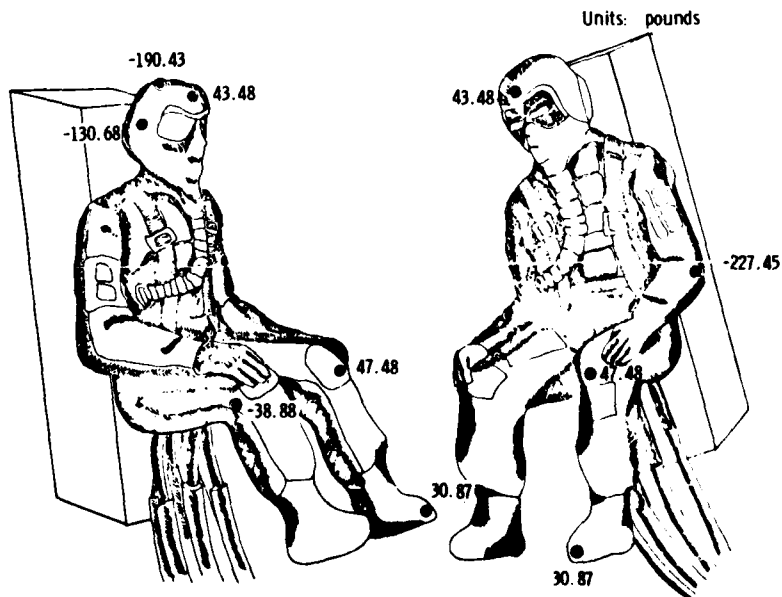


Figure 20. Aerodynamic Loads, WSO, 500 KTS, Sea Level

AERODYN FORCES

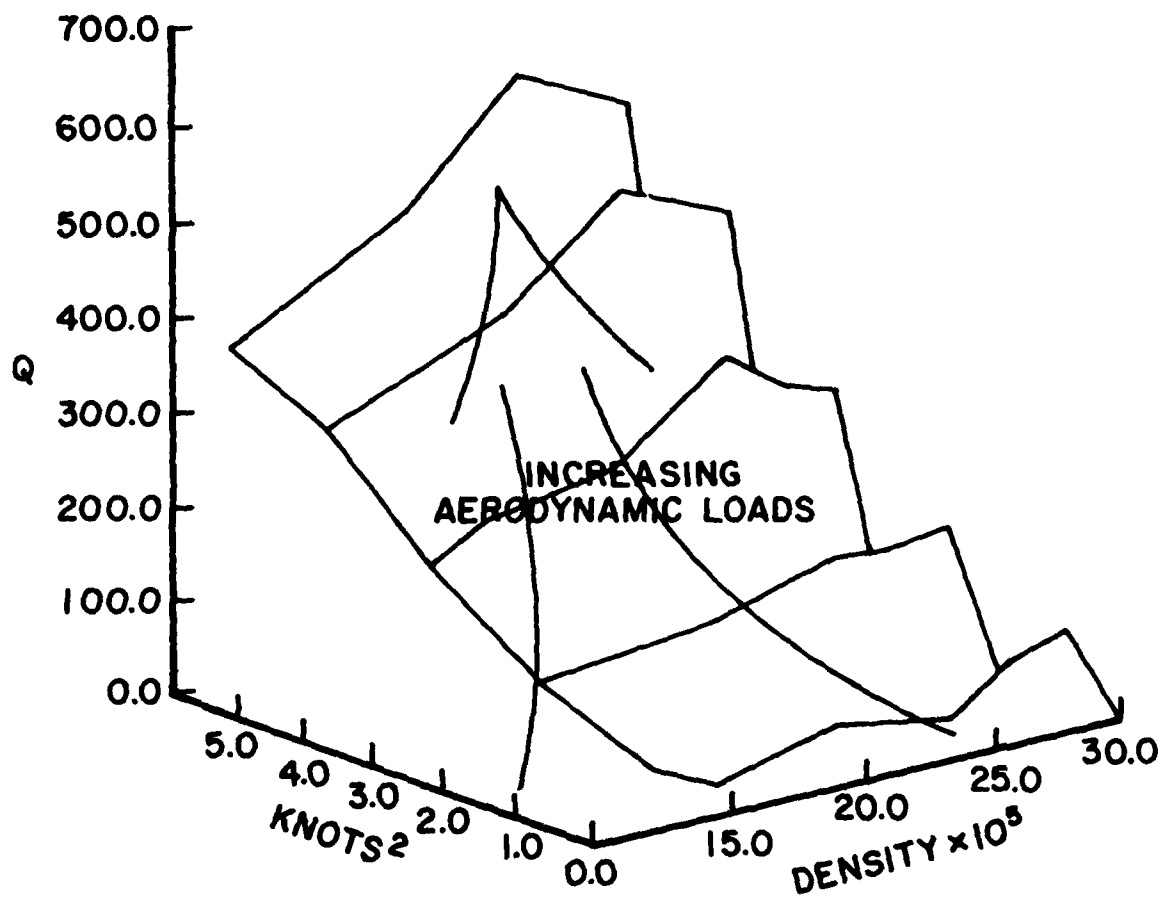


Figure 21. Knots versus Altitude versus "Q"

APPENDIX

Analytic/Graphic Data

The appendix illustrations are the analytical pressure coefficient values measured in the investigation. Pitch values change horizontally and yaw trim attitude varies vertically. Moving from upper-left to lower-right systematically takes the reader from crewmember position 1 through position 4. There are 14 figures included in the Appendix—one for each of seven pressure ports and a group of whole torso values for each of two crewmembers.

		Pitch					
		- 8	- 4	0	4	8	10
Yaw	8	-.349	-.257	-.180	-.174	-.176	-.196
	4	-.277		-.164	-.159	-.158	-.170
	0	-.210	-.202	-.185	-.172	-.172	-.182
	-4	-.255	-.195	-.147		-.147	-.169
	-6	-.267	-.194	-.150	-.147	-.166	-.185

a. Position 1

		Pitch					
		- 8	- 4	- 0	- 4	- 8	- 10
Yaw	8	-.379	-.404	-.397	-.426	-.544	-.565
	4	-.299	-.351	-.336	-.338	-.430	-.567
	0	-.196	-.201	-.268	-.348	-.368	-.363
	-4	-.235	-.275	-.314	-.397	-.476	-.498
	-6	-.262	-.279	-.311	-.374	-.450	-.481

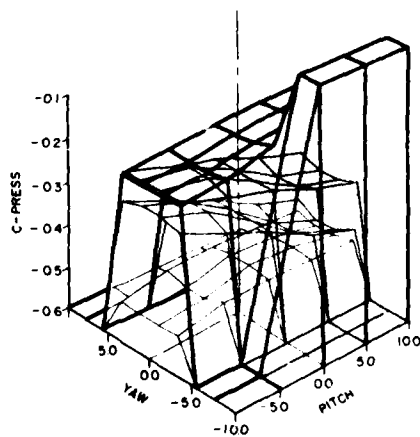
b. Position 2

		Pitch					
		- 8	- 4	- 0	- 4	- 8	- 10
Yaw	8	-.371	-.368	-.378	-.437	-.459	-.467
	4	-.239	-.251	-.331	-.397	-.435	-.452
	0	-.224	-.291	-.356	-.451	-.480	-.507
	-4	-.308	-.286	-.344	-.382	-.435	-.417
	-6	-.326	-.364	-.363	-.413	-.458	-.460

c. Position 3

		Pitch					
		- 8	- 4	- 0	- 4	- 8	- 10
Yaw	8	-.516	-.572	-.546	-.519	-.522	-.546
	4	-.495	-.528	-.505	-.504		-.566
	0	-.589	-.525	-.451	-.463	-.490	-.520
	-4	-.386	-.412	-.422	-.456	-.493	-.533
	-6	-.365	-.440	-.458	-.489	-.522	

d. Position 4



1.1.5 - 1.1.8

Figure 22. Pressure Coefficients, Pilot, PP1

		Pitch					
		- 8	- 4	0	4	8	10
Yaw	8	-.176	-.081	-.092	-.119	-.140	.167
	4	-.111		-.071	-.092	-.121	-.140
	0	-.141	-.034	-.049	-.084	-.118	-.133
	-4	-.036	-.029	-.051		-.103	-.158
	-6	-.059	-.040	-.070	-.106	-.148	-.170

a. Position 1

		Pitch					
		- 8	- 4	0	4	8	10
Yaw	8	-.107	-.165	-.272	-.367	-.444	-.509
	4	-.106	-.196	-.242	-.357	-.459	-.481
	0	-.186	-.328	-.412	-.539	-.725	-.824
	-4	-.434	-.538	-.704	-.875	-1.103	-1.214
	-6	-.505	-.618	-.707	-.802	-.982	-1.096

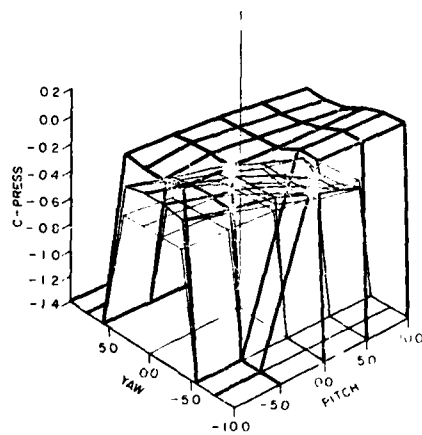
b. Position 2

		Pitch					
		- 8	- 4	0	4	8	10
Yaw	8	-.140	-.268	-.426	-.489	-.807	-1.0
	4	-.140	-.258	-.368	-.493	-.697	-.744
	0	-.210	-.330	-.454	-.637	-.691	-.719
	-4	-.473	-.502	-.615	-.702	-.749	-.5
	-6	-.641	-.772	-.890	-.993	-1.077	-1.11

c. Position 3

		Pitch					
		- 8	- 4	0	4	8	10
Yaw	8	-.183	-.284	-.377	-.519	-.533	-.576
	4	-.231	-.351	-.447	-.504		-.585
	0	-.815	-.490	-.515	-.546	-.603	-.623
	-4	-.691	-.757	-.852	-.941	-1.070	
	-6	-.664	-.788	-.912	-1.029	-1.169	-1.202

d. Position 4



1.25 - 1.28

Figure 23. Pressure Coefficients, Pilot, PP2

		Pitch					
		-8	-4	0	4	8	10
Yaw	8	.228	.029	-.040	-.089	-.125	-.156
	4	.021		-.022	-.066	-.107	-.125
	0	.302	.113	-.016	-.064	-.099	-.123
	-4	.095	0.00	-.026		-.081	-.140
	-6	.077	-.004	-.040	-.084	-.125	-.148

a. Position 1

		Pitch					
		-8	-4	0	4	8	10
Yaw	8	.809	.746	.676	.607	.522	.483
	4	.839	.782	.711	.651	.570	.533
	0	.838	.789	.721	.652	.598	.574
	-4	.816	.766	.700	.632	.576	.546
	-6	.771		.648	.586	.520	.481

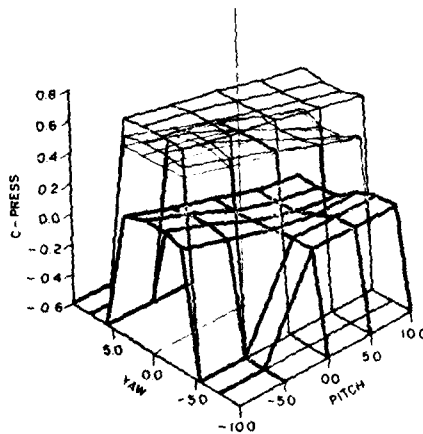
b. Position 2

		Pitch					
		-8	-4	0	4	8	10
Yaw	8	.743	.654	.544	.422	.296	.23
	4	.787	.712	.618	.518	.402	-.4
	0	.746	.660	.572	.422	.299	.236
	-4	.744	.667	-.189	.441	.328	.50
	-6	.707	.621	.516	.402	.280	.224

c. Position 3

		Pitch					
		-8	-4	0	4	8	10
Yaw	8	.751	.657	.538	.407	.283	.201
	4	.791	.697	.586	.467	.301	.261
	0	.758	.657	.550	.424	.299	.225
	-4	.759	.607	.504	.368	.250	.180
	-6	.688	.568	.458	.346	.217	0

d. Position 4



1.35 - 1.38

Figure 24. Pressure Coefficients, Pilot, PP3

		Pitch					
		- 8	- 4	0	4	8	10
Yaw	8	.018	-.015	-.062	-.104	-.140	-.167
	4	.033		-.048	-.085	-.118	-.144
	0	.020	-.005	-.044	-.084	-.118	-.138
	-4	-.018	-.040	-.055		.015	-.151
	-6	-.033	-.048	-.066	-.099	-.137	-.159

a. Position 1

		Pitch					
		- 8	- 4	0	4	8	10
Yaw	8	-.103	-.154	-.107	-.144	-.170	-.181
	4	-.157	-.026	-.051	-.081	-.119	-.137
	0	0.0	-.01	-.039	-.069	-.103	-.127
	-4	0.0	-.022	-.046	-.088	-.118	-.144
	-6	-.018	-.029	-.062	-.092	-.125	-.148

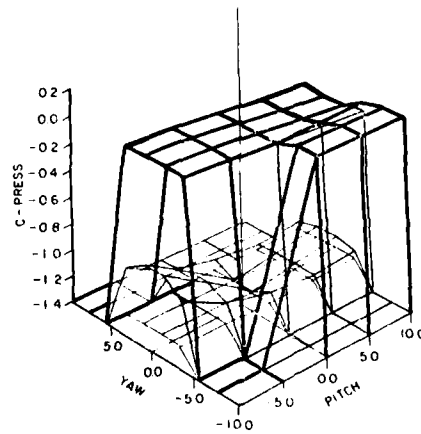
b. Position 2

		Pitch					
		- 8	- 4	0	4	8	10
Yaw	8	-.956	-1.169	-1.241	-1.093	-.852	-.793
	4	-.522	-.653	-.86	-.636	-.587	-.619
	0	-.620	-.098	-.808	-1.172	-1.123	-1.084
	-4	-.549	-.890	-1.022	-.89	-.911	-.667
	-6	-.267	-.460	-.839	-1.052	-.993	-.868

c. Position 3

		Pitch					
		- 8	- 4	0	4	8	10
Yaw	8	-.392	-1.247	-1.209	-1.133	-1.074	-1.082
	4	-.198	-1.236	-1.333	-1.276		-1.213
	0	-.837	-1.206	-1.203	-1.229	-1.216	-1.206
	-4	-.956	-1.151	-1.107	-1.055	-1.176	-1.213
	-6	-.920	-1.147	-1.132	-1.121	-1.199	

d. Position 4



1.45 - 1.48

Figure 25. Pressure Coefficients, Pilot, PP4

		Pitch					
		- 8	- 4	0	4	8	10
Yaw	8	.004	-.022	-.066	-.119	-.158	-.185
	4	.026		-.052	-.100	-.14	-.162
	0	.137	-.005	-.044	-.079	-.113	-.138
	-4	.044	-.007	-.051		-.010	-.169
	-6	.033	-.007	-.059	-.106	-.151	-.178

a. Position 1

		Pitch					
		- 8	- 4	0	4	8	10
Yaw	8	0.0	-.029	-.066	-.104	-.133	-1.51
	4	.026	-.015	-.040	-.07	-.107	-.126
	0	.039	.005	-.029	-.064	-.093	-.113
	-4	.026	-.004	-.036	-.074	-.107	-.125
	-6	.029	-.015	-.048	-.084	-.118	-.133

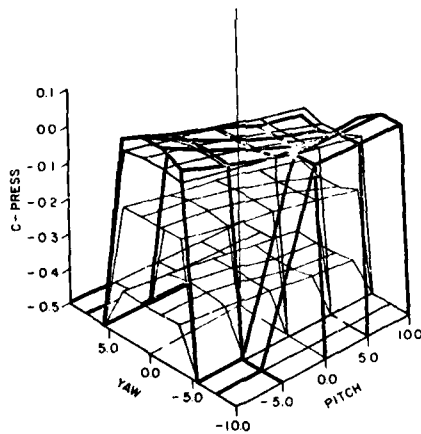
b. Position 2

		Pitch					
		- 8	- 4	0	4	8	10
Yaw	8	-.412	-.216	-.196	-.174	-.174	-.167
	4	-.04	-.063	-.088	-.118	-.107	-.126
	0	-.380	-.365	-.166	-.441	-.446	-.453
	-4	-.399	-.440	-.489	-.438	-.358	-.500
	-6	-.363	-.368	-.381	-.443	-.413	-.386

c. Position 3

		Pitch					
		- 8	- 4	0	4	8	10
Yaw	8	-.037	-.376	-.392	-.407	-.397	-.413
	4	-.205	-.221	-.231	-.25		-.287
	0	-.130	-.127	-.170	-.200	-.245	-.265
	-4	-.096	-.158	-.230	-.287	-.298	-.287
	-6	-.23	-.253	-.275	-.272	-.25	

d. Position 4



1.55 - 1.58

Figure 26. Pressure Coefficients, Pilot, PP5

		Pitch					
		- 8	- 4	0	4	8	10
Yaw	8	.022	-.015	-.059	-.1	-.14	.163
	4	.03		-.045	-.085	-.118	-.140
	0	.112	0.0	-.038	-.084	-.113	-.123
	-4	.015	-.018	-.048		-.020	-.138
	-6	.004	-.018	-.059	-.095	-.129	-.147

a. Position 1

		Pitch					
		- 8	- 4	0	4	8	10
Yaw	8	.007	-.011	-.051	-.096	-.130	-.144
	4	.011	-.011	-.047	-.074	-.107	-.126
	0	.01	-.025	-.049	-.069	-.098	-.118
	-4	-.007	-.059	-.032	-.077	-.107	-.129
	-6	0.0	-.048	-.092	-.081	-.118	-.133

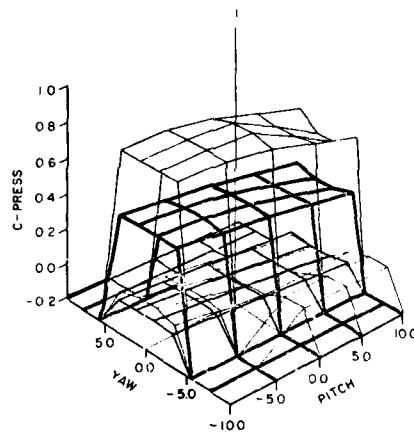
b. Position 2

		Pitch					
		- 8	- 4	0	4	8	10
Yaw	8	.938	.893	.659	.259	.041	.011
	4	-.037	-.037	-.051	-.074	-.107	-.119
	0	.815	.833	-.070	.725	.544	.453
	4	.81	.821	.641	.397	.144	.75
	6	.582	.621	.678	.683	.557	.393

c. Position 3

		Pitch					
		- 8	- 4	0	4	8	10
Yaw	8	.773	.705	.634	.541	.452	.390
	4	.692	.638	.575	.504		.353
	0	.556	.471	.443	.361	.299	.262
	-4	.176	.184	.219	.180	.107	.085
	-6	-.022	-.004	-.018	0.00	-.037	

d. Position 4



1.65 - 1.68

Figure 27. Pressure Coefficients, Pilot, PP6

		Pitch					
		- 8	- 4	0	4	8	10
Yaw	8	.037	-.015	-.044	-.085	-.118	-.144
	4	.048		-.030	-.066	-.103	-.122
	0	-.044	.010	-.022	-.064	-.099	-.123
	-4	.051	.007	-.026		.030	-.129
	-6	.040	.007	-.037	-.077	-.114	-.133

a. Position 1

		Pitch					
		- 8	- 4	0	4	8	10
Yaw	8	.022	-.004	-.044	-.089	-.122	-.140
	4	.033	0.0	-.061	-.062	-.096	-.122
	0		-.010	-.029	-.059	-.088	-.113
	-4	.037	.007	-.029	-.074	-.103	-.122
	-6	-.004	-.007	-.037	-.077	-.114	-.130

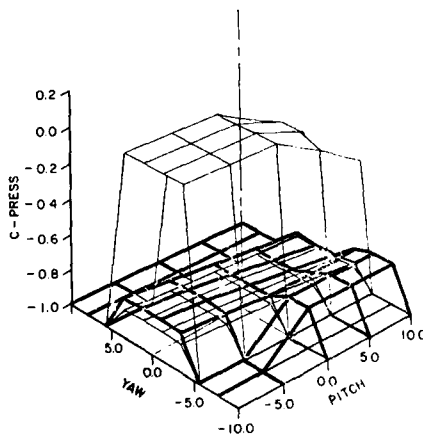
b. Position 2

		Pitch					
		- 8	- 4	0	4	8	10
Yaw	8	-.048	-.066	-.096	-.111	-.137	-.144
	4	-.022	-.044	-.059	-.081	-.092	-.111
	0	-.029	-.049	-.070	-.098	-.108	-.133
	-4	-.026	-.048	-.081	-.103	-.118	-.167
	-6	-.033	-.048	-.084	-.114	-.137	-.14

c. Position 3

		Pitch					
		- 8	- 4	0	4	8	10
Yaw	8	.963	.963	.949	.928	.860	.799
	4	.934	.926	.908	.890		.842
	0	.863	.833	.841	.815	.804	-.191
	-4	.765	.816	.870	.871	.831	.772
	-6	-.146	.634	.685	.721	.743	

d. Position 4



1, 7:5 - 1, 7:8

Figure 28. Pressure Coefficients, Pilot, PP7

		Pitch					
		- 8	- 4	0	4	8	10
Yaw	8	.015	-.064		-.176	-.245	.289
	4		-.039	-.109	-.157		
	0	.015	-.044	-.122	-.157	-.215	
	-4	-.054	-.093	-.013	-.206	-.255	-.304
	-6						

a. Position 1

		Pitch					
		- 8	- 4	0	4	8	10
Yaw	8	-.293	-.382	-.343	-.422	-.422	-.438
	4	-.21	-.230	-.299	-.444	-.343	-.426
	0	-.224	-.298	-.376		-.471	
	-4		-.353	-.451	-.544	-.676	-.662
	-6						

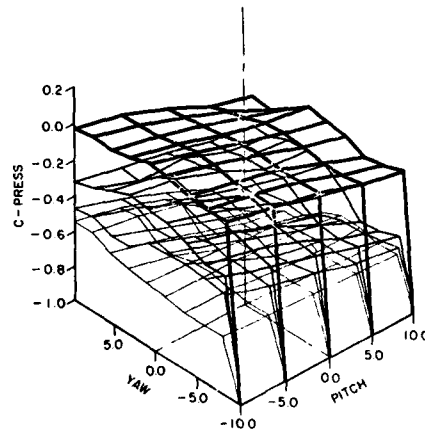
b. Position 2

		Pitch					
		- 8	- 4	0	4	8	10
Yaw	8	-.444	-.515	-.605	-.681	-.740	-.804
	4		-.576	-.683	-.775	-.765	-.779
	0	-.385	-.480	-.554	-.627	-.737	
	-4	-.392	-.529	-.629	-.642	-.667	-.725
	-6						

c. Position 3

		Pitch					
		- 8	- 4	0	4	8	10
Yaw	8	-.534	-.561	-.612	-.735	-.848	-.892
	4	-.613	-.676	-.785	-.794	-.815	-.839
	0	-.654	-.624	-.629	-.603	-.678	
	-4	-.691	-.668	-.709	-.721		
	-6						

d. Position 4



2, 1:1 - 2, 1:4

Figure 29. Pressure Coefficients, WSO, PP1

		Pitch					
		-8	-4	0	4	8	10
Yaw	8	-.005	-.064		-.196	-.25	.289
	4		-.025	-.104	-.157		
	0	.034	-.025	-.093	-.147	-.205	
	-4	0.00	-.054	-0.1	-.176	-.235	-.284
	-6						

a. Position 1

		Pitch					
		-8	-4	0	4	8	10
Yaw	8	-.366	-.618	-.686	-.578	-.515	-.448
	4	-.288	-.304	-.436	-.434	-.544	-.52
	0	-.254	-.322	-.366		-.471	
	-4		-.289	-.363	-.431	-.471	-.471
	-6						

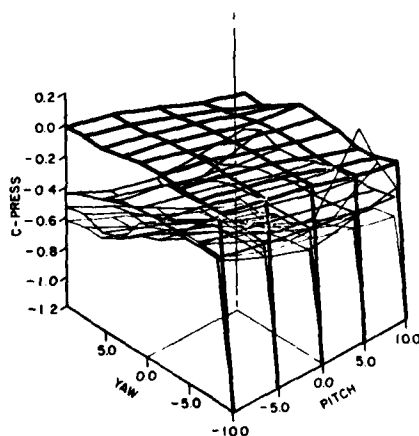
b. Position 2

		Pitch					
		-8	-4	0	4	8	10
Yaw	8	-.488	-.637	-.824	-.961	-1.005	-1.029
	4		-.596	-.723	-.838	-.941	-1.039
	0	-.395	-.539	-.691	-.784	-.941	
	-4	-.245	-.407	-.546	-.652	-.735	.176
	-6						

c. Position 3

		Pitch					
		-8	-4	0	4	8	10
Yaw	8	-.573	-.737	-.869	-.941	-1.029	-1.069
	4	-.544	-.652	-.756	-.828	-.980	-1.02
	0	-.268	-.415	-.561	-.75	-.878	
	-4	-.24	-.337	-.49	-.623		
	-6						

d. Position 4



2.2.1 - 2.2.4

Figure 30. Pressure Coefficients, WSO, PP2

		Pitch					
		- 8	- 4	0	4	8	10
Yaw	8	.034	.01		-.088	-.157	-.186
	4		-.039	-.02	-.069		
	0	.068	.025	.005	.069	.112	
	-4	.049	.015	-.025	-.093	-.137	.176
	-6						

a. Position 1

		Pitch					
		- 8	- 4	0	4	8	10
Yaw	8	.849	.824	.819	.667	.48	.325
	4	.883	.843	.794	.722	.775	.673
	0	.878	.829	.776		.686	
	-4		.784	.716	.657	.598	.588
	-6						

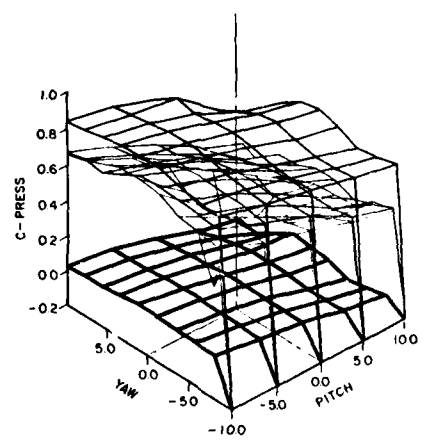
b. Position 2

		Pitch					
		- 8	- 4	0	4	8	10
Yaw	8	.707	.608	.502	.412	.289	.235
	4		.685	.589	.466	.368	.309
	0	.795	.716	.608	.495	.317	
	-4	.765	.676	.566	.451	.343	.284
	-6						

c. Position 3

		Pitch					
		- 8	- 4	0	4	8	10
Yaw	8	.689	.6	.485	-.613	.225	.147
	4	.775	.681	.561	.436	.302	.229
	0	.776	.678	.405	.441	.298	
	-4	.676	.571	.456	.328		
	-6						

d. Position 4



2,3:1 - 2,3:4

Figure 31. Pressure Coefficients, WSO, PP3

		Pitch					
		-8	-4	0	4	8	10
Yaw	8	.049	-.005		-.039	-.093	.078
	4		.01	-.005	-.015		
	0	.059	.010	.005	-.005	-.029	
	-4	.029	.005	0.0	-.044	-.069	-.098
	-6						

a. Position 1

		Pitch					
		-8	-4	0	4	8	10
Yaw	8	.01	0.0	-.098	-.167	-.235	-.281
	4	-.073	-.029	-.142	-.268	-2.84	-3.17
	0	-.122	-.093	-.161		-.333	
	-4		-.142	-.284	-.348	-.373	-.387
	-6						

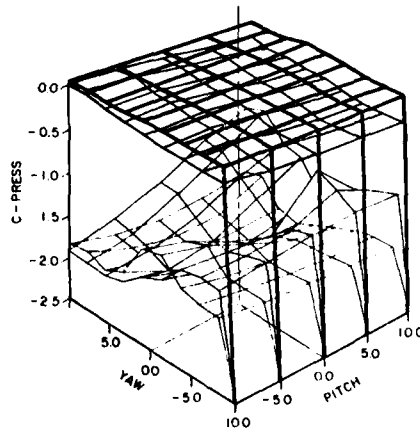
b. Position 2

		Pitch					
		-8	-4	0	4	8	10
Yaw	8	-1.946	-1.828	-1.580	-1.324	-1.034	-1.015
	4		-2.054	-1.946	-1.662	-1.368	-1.289
	0	-1.615	-1.941	-2.054	-1.902	-1.741	
	-4	-1.284	-1.402	-1.522	-.505	-1.289	-1.466
	-6						

c. Position 3

		Pitch					
		-8	-4	0	4	8	10
Yaw	8	-1.743	-2.015	-2.087	-2.103	-1.853	-1.819
	4	-1.804	-2.123	-2.249	-2.299	-2.185	-2.18
	0	-1.176	-1.366	-1.707	-1.987	-2.044	
	-4	-1.578	-1.732	-1.786	-1.858		
	-6						

d. Position 4



2.41 - 2.44

Figure 32. Pressure Coefficients, WSO, PP4

		Pitch					
		- 8	- 4	0	4	8	10
Yaw	8	.054	.02		-.005	-.059	.083
	4		.039	.005	.005		
	0	.073	.034	.01	0.0	-.02	
	-4	.059	.02	.01	-.02	-.039	-.059
	-6						

a. Position 1

		Pitch					
		- 8	- 4	0	4	8	10
Yaw	8	.054	.034	0.0	-.039	-.049	-.084
	4	.083	.069	.02	0.0	-.074	-.079
	0	.102	.068	.044		-.078	
	-4		.069	.044	-.005	-.069	-.098
	-6						

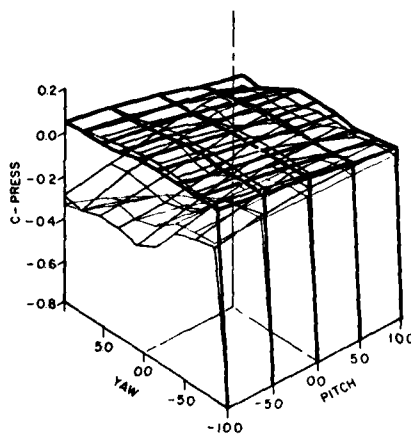
b. Position 2

		Pitch					
		- 8	- 4	0	4	8	10
Yaw	8	-.311	-.366	-.447	-.637	-.598	-.608
	4	-.172	-.216	-.356	-.412	-.454	-.478
	0	-.200	-.21	-.293	-.299	-.268	
	-4	-.108	-.083	-.083	-.054		
	-6						

c. Position 3

		Pitch					
		- 8	- 4	0	4	8	10
Yaw	8	-.332	-.216	-.171	-.098	-.098	-.108
	4		-.281	-.228	-.152		-.118
	0	-.341	-.235	-.167	-.123	-.118	
	-4	-.157	-.069	-.005	0.0	-.039	-.064
	-6						

d. Position 4



2.5.1 - 2.5.4

Figure 33. Pressure Coefficients, WSO, PP5

		Pitch					
		- 8	- 4	0	4	8	10
Yaw	8	.039	.01		-.034	-.088	-.098
	4		.029	.005	-.015		
	0	.059	.029	.01	-.015	-.049	
	-4	.044	.02	.02	-.025	-.064	-.093
	-6						

a. Position 1

		Pitch					
		- 8	- 4	0	4	8	10
Yaw	8	.068	.039	-.005	-.059	-.113	-.143
	4	.093	.064	.02	.01	-.059	-.109
	0	.083	.068	.044		-.039	
	-4		.049	.029	0.0	-.039	-.088
	-6						

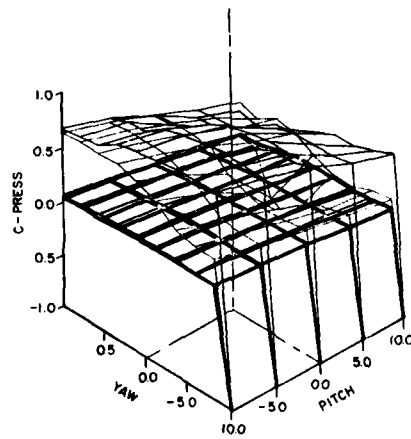
b. Position 2

		Pitch					
		- 8	- 4	0	4	8	10
Yaw	8	.688	.652	.444	.240	.127	.078
	4		.768	.634	.343	.167	.137
	0	.839	.824	.775	.657	.2	
	-4	.863	.828	.766	.569	.392	.289
	-6						

c. Position 3

		Pitch					
		- 8	- 4	0	4	8	10
Yaw	8	.655	.571	.456	.343	.240	.147
	4	.662	.569	.459	.343	.249	.185
	0	.576	.454	.356	-.735	.122	
	-4	.304	.21	.102	-.015		
	-6						

d. Position 4



2.61 - 2.64

Figure 34. Pressure Coefficients, WSO, PP6

		Pitch					
		-8	-4	0	4	8	10
Yaw	8	.063	.049		.01	-.039	-.044
	4		.069	.045	.029		
	0	.063	.064	.049	.029	0.0	
	-4	.074	.059	.055	.02	-.01	-.029
	-6						

a. Position 1

		Pitch					
		-8	-4	0	4	8	10
Yaw	8	.063	.064	.049	.034	0.0	-.015
	4	.093	.088	.069	.049	.02	-.005
	0	.098	.093	.073		.02	
	-4		.088	.069	.044	.02	-.005
	-6						

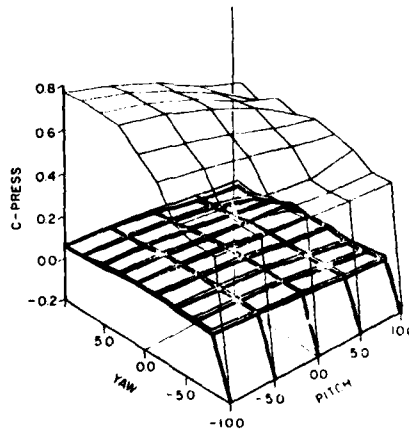
b. Position 2

		Pitch					
		-8	-4	0	4	8	10
Yaw	8	.068	.059	.039	.029	-.005	-.015
	4		.084	.074	.049	.02	0.0
	0	.093	.083	.069	.049	0.0	
	-4	.078	.069	.054	.025	.005	-.01
	-6						

c. Position 3

		Pitch					
		-8	-4	0	4	8	10
Yaw	8	.786	.727	.650	.569	.475	.431
	4	.779	.735	.668	.608	.512	.434
	0	.663	.61	.571	.515	.454	
	-4	.426	.415	.383	.363		
	-6						

d. Position 4



2.7:1 - 2.7:4

Figure 35. Pressure Coefficients, WSO, PP7

REFERENCES

- Arnold, L., *Dynamic Measurements in Wind Tunnels*. AGARDograph 11, 1955.
- Combs, S. P. *Correlation of Mechanism of Extremity Injury and Aerodynamic Factors in Ejections from F-4 Aircraft*. AMRL-TR-78-62 (AD A064642), Aerospace Medical Research Laboratory, Wright-Patterson AFB, OH, 1978.
- Dabold, J. L., *A Wind Tunnel Investigation of Aerodynamic Effects of BIAS Light Pods on the C-130 Aircraft*. Thesis. Air Force Institute of Technology, Wright-Patterson AFB, Ohio, 1971.
- Grevel, R. J., *Static Stability Test of a Plastic Model X-15 in the Institute of Technology 13.5 Inch Wind Tunnel*. Thesis. Air Force Institute of Technology, Wright-Patterson AFB, Ohio, 1969.
- Grunhofer, H. J. and Kroh, G. A. *Review of Anthropometric Data of German Air Force and United States Air Force Flying Personnel, 1967-1968*.
- Haebec, G. F. and Dunn, H. J., *Instrumentation and Calibration of a Low-Speed Wind Tunnel*. Thesis GAE-55. Air Force Institute of Technology, Wright-Patterson AFB, Ohio, 1955.
- Kazarian, L. Belk, W. and Hoffman, H. *Traumatic Lesions of the Cervical Spine, 1971-1979: Incidence-Severity and Classification*. Aerospace Medical Panel of AGARD NATO, Bodo, Norway, May 1980.
- Knackstedt, W. F. and Sury, J. J., *Spin and Recovery Test of a 1/20 - Scale Model of a Cessna XT-37 Airplane*. Thesis. Air Force Institute of Technology, Wright-Patterson AFB, Ohio, 1957.
- Lynch, G. P., *A Low Speed Wind Tunnel Investigation of a F-86A Model*. Thesis GAM 66A/AE/66-4 Air Force Institute of Technology, Wright-Patterson AFB, Ohio, 1966.
- McDonnell and Douglas Corporation, *Part Eight: Miscellaneous Loads*. Report 8718, 1963.
- Morehouse, G. G., *Spin Investigation of a 1/25-Scale Model of the F-86D Airplane*. WADC TR 54-171, Wright Air Development Center, Wright-Patterson AFB, Ohio, 1954.
- Owen, D. H., *Wind Tunnel Test Comparison of a Commercial Plastic Model F106 with a Precision Scale Model F106*. Thesis. Air Force Institute of Technology, Wright-Patterson AFB, Ohio, 1958.
- Pankhurst, R. C. and Holder, D. W., *Wind-Tunnel Technique*. Sir Isaac Pitman and Sons, LTD, London, 1952.
- Poe, A., *Wind-Tunnel Testing*. John Wiley and Sons, Inc., New York, 1954.
- Pope, A., *Wind Tunnel Calibration Techniques*. AGARDograph 54, 1961.
- Skujins, M., *C-141 Wind Tunnel Performance Evaluation*. Flight Test Report ENE FTR 75-7, Aeronautical Systems Division, Wright-Patterson AFB, Ohio, 1975.
- Taylor, D. W., *Some Aspects of the Comparison of Model and Full-Scale Tests*. *National Advisory Committee for Aeronautics - Report No. 219*, Washington, 1926.
- Wood, R. B., *The Instrumentation and Calibration of the AFIT Cascade Wind Tunnel*. Thesis. Air Force Institute of Technology, Wright-Patterson AFB, Ohio, 1957.

ATE
MED
-8